GE-NE-B13-01739-04
Revision 0
Class III
DRF B13-01739

Nine Mile Point Unit 1 Shroud Repair Hardware Stress Analysis

January, 1995

Prepared by:

Gary L. Stevens 1/18/95
G. L. Stevens, Senior Engineer
Structural Mechanics Projects

K. Karim-Panahi 1/18/95
K. Karim-Panahi, Principal Engineer
Structural Mechanics Projects

T.A. Haveliwala 1/18/95
T. A. Haveliwala, Engineer
Structural Mechanics Projects

Sofia Zaliznyak 1/18/95
S. Zaliznyak, Engineer
Structural Mechanics Projects

Verified by:

S.T. Hlavaty 1/18/95
S. T. Hlavaty, Engineer
Structural Mechanics Projects

M. Kaul 1/18/95
M. Kaul, Principal Engineer
Structural Mechanics Projects

Approved by:

1-18-95
P. J. Walier, Project Manager
Nine Mile Point 1 Shroud Repair Project

GE Nuclear Energy

IMPORTANT NOTICE REGARDING CONTENTS OF THIS REPORT

Please Read Carefully

This report was prepared by General Electric solely for the use of the Niagara Mohawk Company. The information contained in this report is believed by General Electric to be an accurate and true representation of the facts known, obtained or provided to General Electric at the time this report was prepared.

The only undertakings of the General Electric Company respecting information in this document are contained in the contract governing this work, and nothing contained in this document shall be construed as changing said contract. The use of this information except as defined by said contract, or for any purpose other than that for which it is intended, is not authorized; and with respect to any such unauthorized use, neither General Electric Company nor any of the contributors to this document makes any representation or warranty (express or implied) as to the completeness, accuracy or usefulness of the information contained in this document or that such use of such information may not infringe privately owned rights; nor do they assume any responsibility for liability or damage of any kind which may result from such use of such information.

PROPRIETARY INFORMATION NOTICE

This document contains proprietary information of the General Electric Company and is furnished to the Niagara Mohawk Company in confidence solely for the purpose or purposes stated in the contract between the Niagara Mohawk Company and the General Electric Company. The Niagara Mohawk Company shall not publish or otherwise disclose this document or the information to others without the written consent of the General Electric Company except as provided in such contract, and shall return this document at the request of the General Electric Company.

Proprietary information contained in this report is designated by "bars" located in the right hand margin.

TABLE OF CONTENTS

Page No.

TABLE OF CONTENTS (cont'd)

Page No.

LIST OF FIGURES

LIST OF FIGURES (cont'd)

LIST OF TABLES

LIST OF TABLES (cont'd)

1.0 INTRODUCTION

The Nine Mile Point Unit 1 (NMP-1) core shroud contingency repair is designed to structurally replace circumferential shroud welds H1 through H7. The shroud weld locations are shown in Figure 1-1. The shroud repair also includes a feature that addresses a postulated failure of bi-metallic weld H8 that joins the stainless steel shroud support ring with the Inconel shroud support cone. The repair is designed in accordance with the criteria set forth in BWROG VIP Core Shroud Repair Design Criteria, Revision 1, September 12, 1994.

The NMP-1 repair of the core shroud is considered a non-ASME code repair and therefore is performed as an alternative to ASME Section XI as permitted by 10CFR50.55a(a)(3). The upper and lower repair hardware for the NMP-1 shroud is shown in Figures 1-2 and 1-3 respectively. The complete repair hardware assembly with all components installed is shown in Figure 1-4. The repair consists of a tie rod assembly and weld H8 support brackets.

1.1 Tie Rod Assembly Description

The shroud repair for NMP-1 consists of four (4) symmetrically placed tie rod assemblies located in the shroud RPV annulus. Each tie rod assembly has lateral springs attached at the top guide and the core plate elevations to provide lateral support to the shroud. These lateral springs transfer the horizontal load between the shroud and the RPV. Each tie rod assembly also has a lateral rigid stabilizer located at the central elevation of the shroud to provide lateral support of the central shroud cylinder in the event of multiple failure of welds H4 and H5. Each tie rod assembly also incorporates an axial spring which provides axial flexibility to accommodate postulated temperature transients.

The ends of the tie rod assemblies are attached to the shroud head and the Inconel shroud conical support at the top and bottom of the tie rod assemblies, respectively. The shroud head is notched at four azimuthal locations (eight notches) using electric discharge machining (EDM) to accommodate the installation of the upper stabilizer support (see Appendix B for structural evaluation of these notches). At the bottom, two holes are machined through the angled Inconel conical support for attaching each tie rod assembly to the conical support using two toggle bolts.

1.2 Weld H8 Support Bracket Description

The tie rod assemblies are designed to carry all of the design loads if welds H1 through H7 are severed. However, additional support is required at the bottom of the shroud in the event of H8 weld failure. The shroud is therefore supported by six (6) bracket supports located at azimuthal locations between tie rod locations. Each of the six bracket supports consist of an upper and lower bracket. Four holes are machined through the shroud above weld H7. The upper bracket is attached to the shroud by the four holes using two toggle bolts and two shear keys. The lower bracket rests on the Inconel conical support and bears against the vessel wall, and is held in place by the ears of the upper bracket. Any potential stagnant flow conditions to the H9 vessel attachment weld caused by the addition of the H8 weld bracket were considered in the design and found to be acceptable (Reference 9).

1.3 Analysis Description

This report presents the detailed stress analysis performed for the repair assembly, including the stresses induced in the shroud and conical support by the repair assembly. Extensive stress analysis was performed for all of the shroud repair parts and affected reactor components. This analysis was divided into three separate parts for convenience: (i) the conical support (including the adjacent reactor vessel and weld H9), (ii) the shroud and tie rod assemblies, and (iii) the repair hardware components. Item (i) is addressed in Section 3.0, Item (ii) is addressed in Section 4.0 and Item (iii) is addressed in Section 5.0 of this report. Stresses induced into the vessel wall by the repair hardware are addressed in the Reference 8 report. The stress analysis is conducted consistent with the load categorizations and stress limits specified in Reference 1.

The main purpose of the analysis is to assess the design and performance requirements for the repair assembly. The stresses in the repair assembly were determined as a result of installed preload, seismic and plant operational loads to ensure they remain below the allowable levels identified in Reference 1 for long term plant operation. In addition, stresses induced in the shroud and conical support as a result of the installed assembly were compared to allowable values. The details of the analysis and the results are presented herein.

Figure 1-1: Nine Mile Point 1 Shroud Configuration

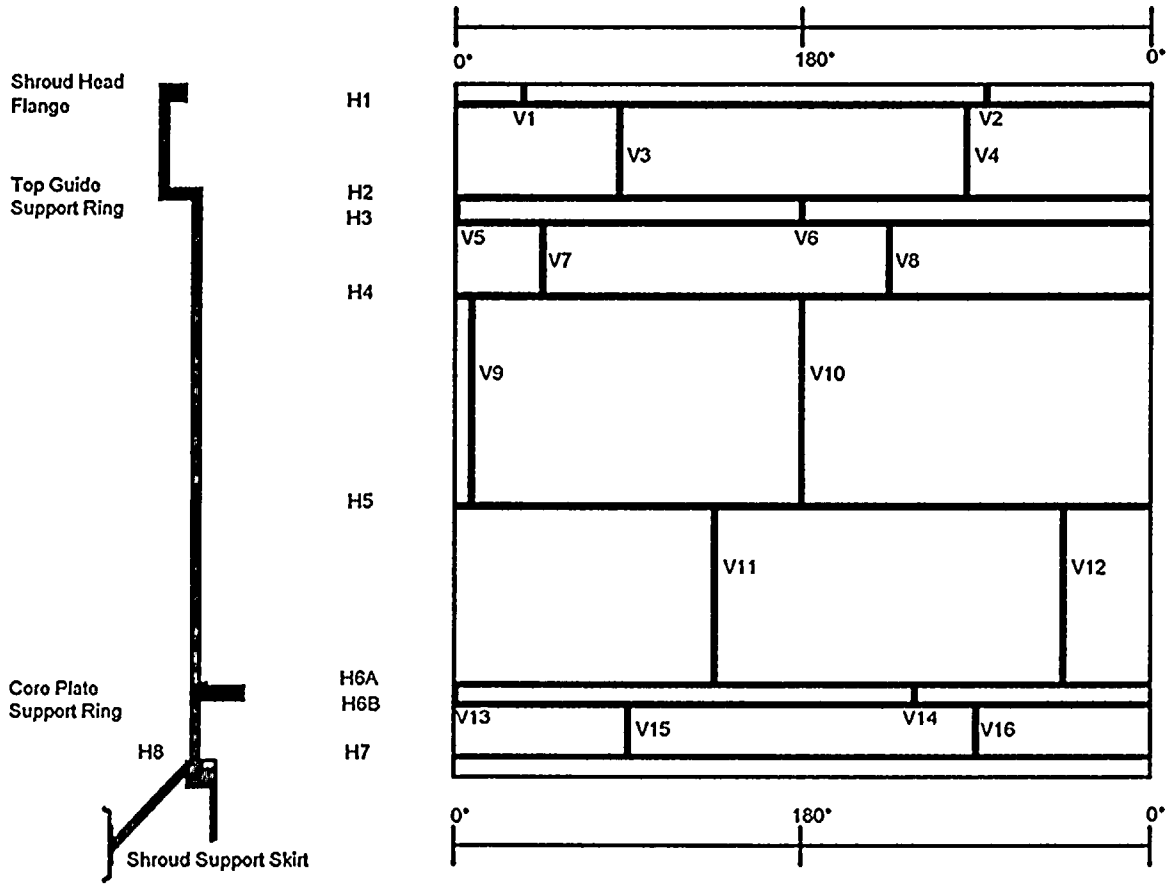

NOT TO SCALE

Figure 1-2: Upper Portion of NMP-1 Shroud Repair Hardware

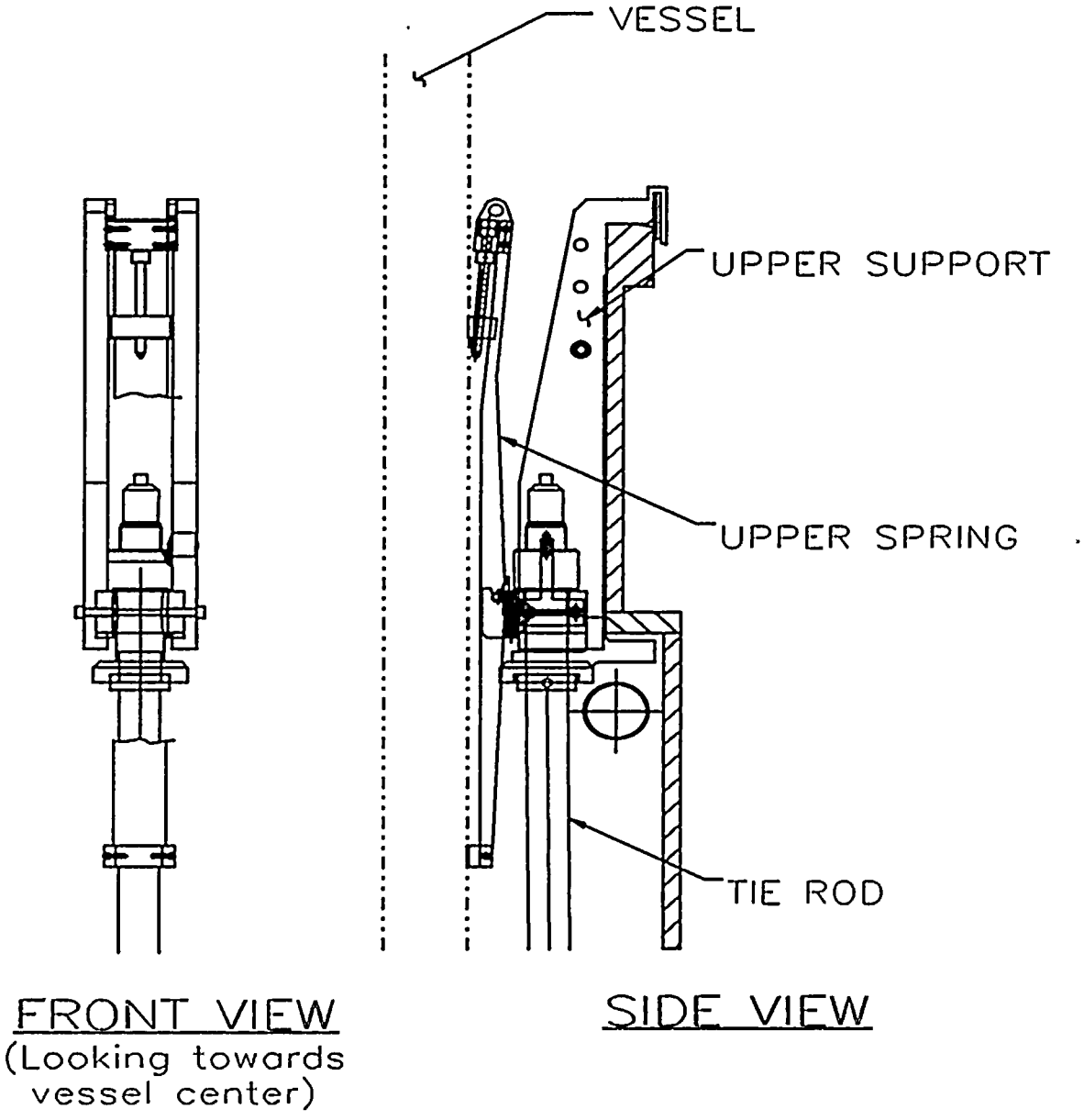

Figure 1-3: Lower Portion of NMP-1 Shroud Repair Hardware

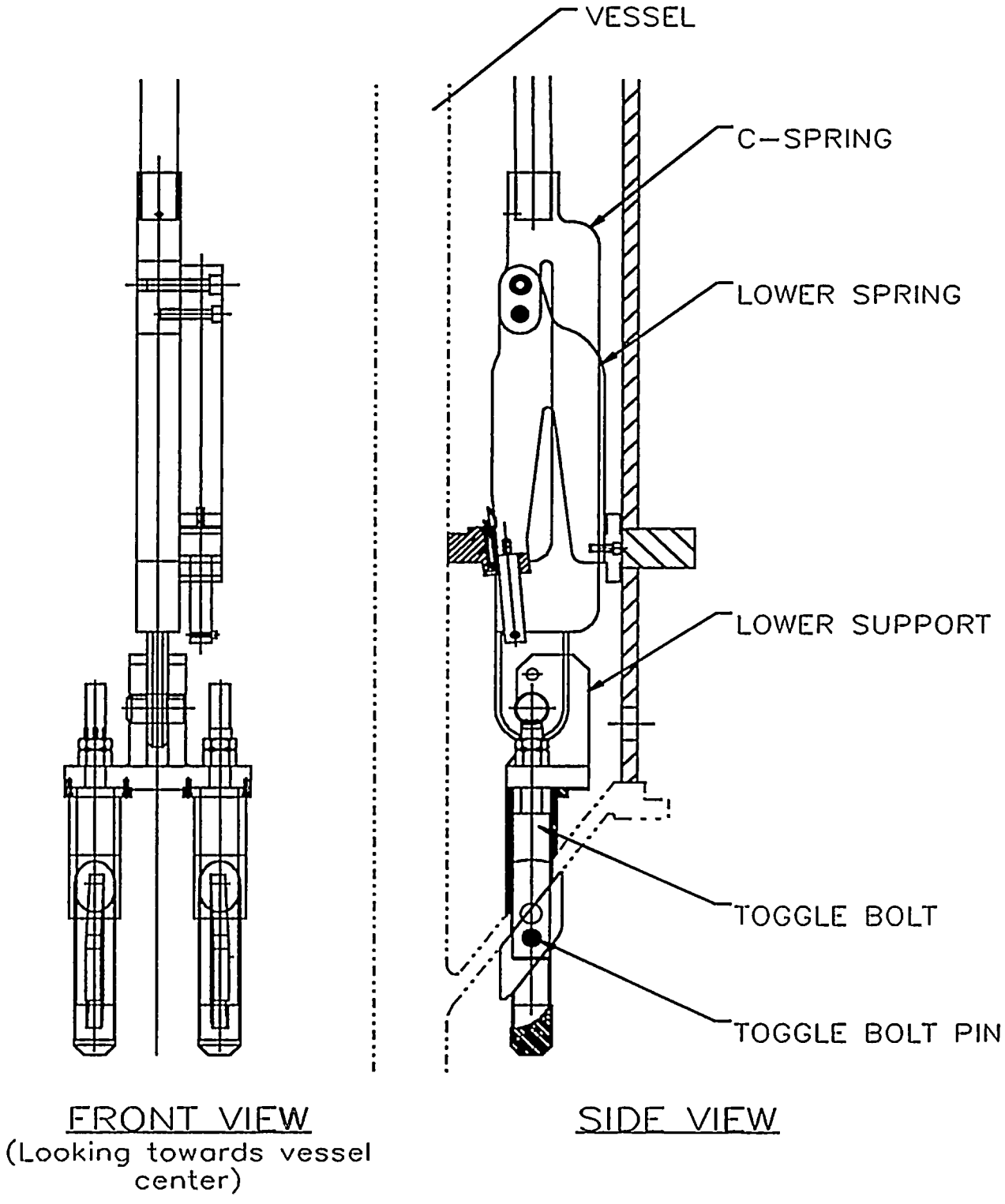

Figure 1-4: NMP-1 Shroud Repair Hardware Assembly

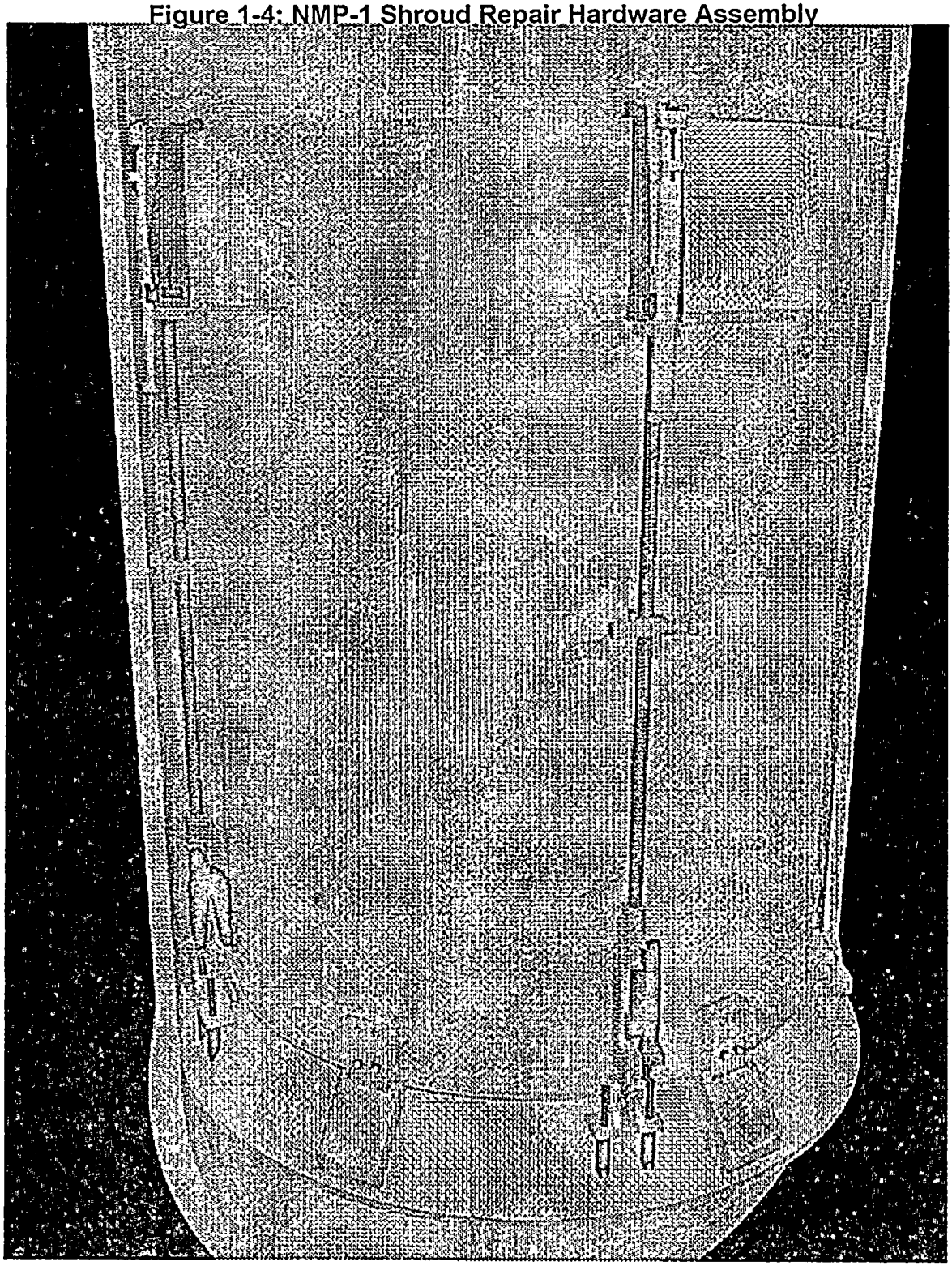

2.0 MATERIAL PROPERTIES AND APPLIED LOADS

This section defines the applied loads, material properties and stress allowables used in the analysis. The definitions and methods outlined in Reference 1 were used as the basis for the values shown in this section.

2.1 Stabilizer Load Summary

The calculations below evaluate the loads and stabilizer load combinations for each event described in the design specification (Reference 1). The limiting stabilizer loads for each event are summarized below.

Event	Bounding Load, lb.
Normal Operation	79,670
Upset (thermal)	188,638
Upset (seismic)	162,076
Emergency	216,520
Faulted	311,710

2.1.1 Component Weights

Component	Weight	Applicable GE Drawing
Shroud Head and Separators	78,000 lb	706E222
Shroud	70,000 lb	706E231
Top Guide	8,900 lb	706E234
Core Support	14,700 lb	706E235
Shroud Head Bolt (36)	10,440 lb	846D690
Peripheral Fuel (16)	10,670 lb	846D634
	Total Weight = 192,710 lb	

Volume of Above Items = 192,710 lb / 0.29 lb/in^3 /1728 in^3/ft^3 = 384 ft^3

Buoyancy of Above Items = 384 ft^3/ 0.0216 ft^3/lb= 17,800 lb
(specific volume of water = 0.0216 ft^3/lb)

Net Weight = 192,710 - 17,800 = 174,910 lb

The net weight acts against the upward pressure loads and is distributed among the four stabilizer assemblies. The effect of the net weight on each stabilizer is 174,910 lb / 4 = 43,727 lb.

In the event of a recirculation line LOCA, only the shroud head and separators act against the ΔP loads across the shroud head.

Shroud head weight = 78,000 lb
Shroud head volume = 78,000 lb / 0.29 lb/in^3 / 1728 in^3/ft^3 = 155 ft^3
Buoyancy = 155 ft^3 / 0.016 ft^3/lb = 9690 lb
Net weight = 78,000 lb - 9690 lb = 68,300 lb
Net affect per stabilizer = 68,300lb / 4 = 17,080 lb

2.1.2 Pressure Loads

The reactor pressure loads act on different areas to contribute to the tie rod loads. The areas considered for this analysis are listed below.

Core support area = $\pi/4 \times [172^2 - (129 \times 12.875^2)]$ = 11,253 in^2

Core support to shroud annulus area = $\pi/4 \times (176^2 - 172^2)$ = 1093 in^2

Total area at core support = Acs = 12,346 in^2

Total shroud head area = $\pi/4 \times 184^2$ = 26,590 in^2

Net shroud head area = Ash = $\pi/4 \times 176^2$ = 24,328 in^2
(less top guide ring)

During normal, upset and most emergency and faulted events the pressure results in an upward load across the core support and shroud head. The stabilizers resist the upward loads produced by the core support, ΔPcs, and the shroud head, ΔPsh. The pressure contribution to stabilizer loads for each event is shown in the table below. In the event of a recirculation line LOCA, the negative (downward) pressure across the core does not contribute to the stabilizer loads, but the shroud head pressure does. Assuming a failed H1 weld, the weight acting against the pressure load in this case is only that of the shroud head and separators. The stabilizer load is one fourth of the total load. The table below gives the normal and upset ΔP's at 105% core flow conditions.

Table 2-1: Pressure Loads

Event	ΔPcs (psi)	ΔPsh (psi)	Total ΔP Load (lb)	Stabilizer ΔP Load (lb)
Normal	15.9	5.9	339,836	84,959
Upset	18.3	8.9	442,451	110,613
Steam Line LOCA	41	22	1,041,000	260,250
Recirc. Line LOCA	-132	7	186,130	46,530

2.1.3 Seismic Loads

The seismic events contribute to stabilizer loads by acting against the over-turning moment and by restraining the vertical load. The resistance to the over-turning moment is assumed to be carried by one stabilizer assembly and the vertical seismic contribution is assumed to be distributed by the four stabilizer assemblies. The maximum stabilizer load acting against the moment is 92,000 lb. The vertical acceleration during a seismic event is 0.073g.

Total vertical seismic load = 0.073 x 174,910 = 12,770 lb

This load is assumed divided evenly among the four stabilizers, or 3190 lb per stabilizer assembly .

Total seismic load per stabilizer = 92,000 lb + 3190 lb = 95,190 lb

2.1.4 Stabilizer Stiffness

The upper support, tie rod, and the C-spring all contribute to the stiffness of the tie rod assembly. Except for the tie rod, the stiffness of the individual components are determined from the finite element analysis of the parts. The stiffness values are listed below.

Upper support = k_b =1.53 x 10^6 lb/in

C-spring stiffness = k_s =1.36 x 10^6 lb/in

Tie rod stiffness = k_r = AE/L = (π/4 x3.5^2) x 25.8 x 10^6 / 136.6 = 1.8 x 10^6 lb/in

A = tie rod area = π/4 x 3.5^2 = 9.62 in^2
E = modulus of elasticity = 25.8 x 10^6 psi
L = tie rod length = 136.6 in.

The net assembly stiffness, k_a is :

$$1/k_a = 1/k_b + 1/k_s + 1/k_r$$

$$k_a = 514{,}000 \text{ lb/in}$$

2.1.5 Thermal Loads

During normal operation the tie rod is at the annulus temperature which is the same as the reactor inlet temperature of 515°F (maximum). The shroud temperature varies from the 515°F inlet temperature to the 546°F reactor outlet, for an average temperature of 530°F. The tie rod assembly includes 136.6 inches of 316L stainless steel and a total of 114.25 inches of Inconel X-750. The shroud includes 238 inches of 304 stainless steel and 12.8 inches of the Inconel cone. The temperatures and material combinations result in differential thermal growth putting the tie rod in tension and the shroud in compression.

Shroud thermal growth = 238" x 9.76×10^{-6} in/in-°F x (530°F - 70°F) =	1.068 in
Cone thermal growth = 12.8" x 7.65×10^{-6} in/in-°F x (530°F - 70°F) =	0.045 in
Shroud total growth =	1.113 in

Tie rod thermal growth = 136.6" x 9.50×10^{-6} in/in-°F x (515°F - 70°F) =	0.577 in
Inconel X-750 growth = 114.25" x 7.50×10^{-6} in/in-°F x (515°F - 70°F) =	0.381 in
Stabilizer total growth =	0.958 in

Net differential thermal growth = ΔL = 1.113 in - 0.958 in = 0.155 in

The shroud is assumed much stiffer than the stabilizer assembly and the total differential is assumed to be taken by the flexibility of the stabilizer assembly. This assumption results in conservatively large stabilizer loads.

Stabilizer load = $k_a \times \Delta L$ = 514,000 lb/in x 0.155" = 79,670 lb

The upset thermal condition assumes cold water is introduced into the annulus while the temperature inside the shroud remains at 545°F. This situation could occur with the loss

of feedwater followed by restoring the feedwater flow, but without heating. Typical thermal cycle diagrams for this event show the annulus temperature can reach as low as 300°F. The stabilizer temperature is assumed to be the 300°F annulus temperature and the shroud is assumed to be at 422°F, which is the average of the shroud inside and outside temperatures. The shroud expansion coefficients are for the material at 422°F and the stabilizer expansion coefficients are for the material at 300°F.

Shroud thermal growth = 238" x 9.61×10^{-6} in/in-°F x (422°F - 70°F) =	0.805 in
Cone thermal growth = 12.8" x 7.46×10^{-6} in/in-°F x (422°F - 70°F) =	0.033 in
Shroud total growth =	0.838 in

Tie rod thermal growth = 136.6" x 8.97×10^{-6} in/in-°F x (300°F - 70°F) =	0.282 in
Inconel X-750 growth = 114.25" x 7.20×10^{-6} in/in-°F x (300°F - 70°F) =	0.189 in
Stabilizer total growth =	0.471 in

Net differential thermal growth = ΔL =0.838 - 0.471 = 0.367 in

The shroud is assumed much stiffer than the stabilizer assembly and the total differential is assumed to taken by the flexibility of the stabilizer assembly. This assumption results in conservatively large stabilizer loads.

Stabilizer load = $k_a \times \Delta L$ = 514,000 lb/in x 0.367" = 188,638 lb

2.1.6 Asymmetric Loads

During a recirculation line break, the water rushing out the failed pipe results in an asymmetric load on the shroud. This load is calculated in Reference 7 which includes a 4,500,000 in-lb moment applied to the shroud. The moment is assumed to be restrained by the stabilizers. The load is calculated assuming the shroud is pivoting about its edge and being restrained by a single stabilizer.

Stabilizer load = 4,500,000 in-lb / (179 in + 9 in) = 23,936 lb

2.2 Load Cases

Loads were developed based on the operating condition definitions contained in Reference 1. These loads were applied in the analyses described in Sections 3, 4 and 5, to determine stresses. Nine (9) load cases were evaluated as specified in Reference 1. Table 2-2 summarizes the load cases examined.

Normal Operation (Load Case #1):

Pressure load =	84,959 lb
Net weight =	-43,727 lb
Total =	41,232 lb

The normal thermal preload is 79,670 lb. Since the thermal preload is not exceeded by the pressure load, all of the joints will remain compressed, ~~(i.e., preload is not exceeded)~~. In reality, a portion of the pressure load will be carried by the tie rod in addition to the preload (analogous to a bolted joint under applied loading). However, the thermal preload value shown here was conservatively used as the bounding load for normal operating conditions since it is based on the tie rod absorbing all differential thermal expansion effects (This leads to a more conservative load than if load sharing and the applied load are both accounted for).

Upset 1 (Load Case #2):

Upset 1 includes the upset pressure, weight and upset thermal conditions.

Upset pressure load =	110,613 lb
Net weight =	-43,727 lb
Total =	66,886 lb

Upset thermal load = 188,638 lb

As with the normal condition, the upset thermal preload (same as the normal preload) is not exceeded by the pressure load, so it is used as the bounding load.

Upset 2 (Load Case #3):

Upset 2 includes upset pressure, weight and seismic loads.

Upset Pressure load =	110,613 lb
Net weight	-43,727 lb
Seismic loads	95,190 lb
Total stabilizer load =	162,076 lb

The normal thermal preload of 79,670 lb is exceeded for this event, so the entire pressure/seismic load shown above is carried by the tie rods and was used as the bounding load.

Emergency 1 (Load Case #4):

The loads for Emergency 1 are the same as for Upset 2.

Emergency 2 (Load Case #5):

Emergency 2 includes the steam line LOCA pressure loads and weight.

Pressure loads =	260,250 lb
Net weight =	-43,727 lb
Total load =	216,520 lb

The normal thermal preload of 79,670 lb is exceeded for this event, so the entire pressure load shown above is carried by the tie rods and was used as the bounding load.

Emergency 3 (Load Case #6):

Emergency 3 includes a recirculation line LOCA. For this case, the large ΔP across the core support does not contribute to the stabilizer loads, but the ΔP across the shroud head does. The only weight acting against the pressure is that of the shroud head and separators. This case also includes the asymmetric loads applied to the shroud.

Pressure load =	46,530 lb
Net weight =	-17,080 lb
Asymmetric load =	23,936 lb
Total load =	53,386 lb

As with the normal condition, the Emergency 3 thermal preload (same as the normal thermal load) is not exceeded by the pressure load, so it is used as the bounding load.

Faulted 1 (Load Case #7):

Faulted 1 includes the steam line LOCA pressure, weight and seismic loads.

Pressure loads =	260,250 lb
Net weight =	-43,727 lb
Seismic loads =	95,190 lb
Total load =	311,710 lb

The normal thermal preload of 79,670 lb is exceeded for this event, so the entire pressure/seismic load shown above is carried by the tie rods and was used as the bounding load.

Faulted 2 (Load Case #8):

Faulted 2 includes the recirculation inlet line LOCA, weight and the seismic loads. For this case, the large ΔP across the core support does not contribute to the stabilizer loads, but the ΔP across the shroud head does.

Pressure loads =	46,530 lb
Net weight =	-17,080 lb
Seismic loads =	95,190 lb
Total load =	126,640 lb

The normal thermal preload of 79,670 lb is exceeded for this event, so the entire pressure/seismic load shown above is carried by the tie rods and was used as the bounding load.

Faulted 3 (Load Case #9):

Faulted 3 combines the recirculation outlet line LOCA, weight and the seismic loads. For this case, the large ΔP across the core support does not contribute to the stabilizer loads, but the ΔP across the shroud head does. The asymmetric loads are also included in this event.

Pressure loads =	46,530 lb
Net weight =	-17,080 lb
Seismic loads =	95,190 lb
Asymmetric load =	23,936 lb
Total load =	148,576 lb

The normal thermal preload of 79,670 lb is exceeded for this event, so the entire pressure/seismic load shown above is carried by the tie rods and was used as the bounding load.

2.3 Summary of Material Properties

Constant material properties evaluated at a temperature of 550°F (design temperature from Reference 1) were utilized in the stress analysis, as shown in Table 2-3. Material allowable stress values utilized in the stress analysis are shown in Table 2-4 and allowable stress limits are summarized in Table 2-5.

Table 2-3: Material Properties of Components Analyzed

Property	Description	Material #1 =Conical Support = Inconel 600 = SB 168 = (Ni-Cr-Fe)	Material #2 = Reactor Vessel = Low Alloy Steel = SA 302 Gr. B (Mn-½Mo)	Material #3 = Shroud = 304 SS = SA 240 = (18Cr-8Ni)	Material #4 = Springs, Upper Support & Tie rod = Inconel X-750
ρ	Density	0.29 lb/in^3	0.29 lb/in^3	0.29 lb/in^3	0.29 lb/in^3
E	Modulus of Elasticity	29.4x10^6 psi	27.7x10^6 psi	25.7x10^6 psi	28.85x10^6 psi
μ	Poisson's Ratio	0.3	0.3	0.3	0.3
α	Mean Coefficient of Thermal Expansion	7.65x10^{-6} in/in-°F	7.125x10^{-6} in/in-°F	9.76x10^{-6} in/in-°F	7.50x10^{-6} in/in-°F
k	Thermal Conductivity	0.90 Btu/hr-in-°F	1.9917 Btu/hr-in-°F	0.925 Btu/hr-in-°F	0.733 Btu/hr-in-°F
c	Specific Heat	0.1253 Btu/lb-°F	0.1310 Btu/lb-°F	0.1288 Btu/lb-°F	0.1211 Btu/lb-°F
δ	Thermal Diffusivity	0.172 ft^2/hr	0.364 ft^2/hr	0.172 ft^2/hr	0.145 ft^2/hr

Notes: (1) All values are evaluated at a temperature of 550°F.

Table 2-4: Allowable Stress Values

Component	Material	S_m @ 550°F (ksi)	S_y @ 100°F (ksi)	S_y @ 550°F (ksi)
Conical Support	SB 168 Inconel	23.3(1)	35.0	28.35
H9 Vessel Attachment Weld	SB 168 Inconel	23.3(1)	35.0	28.35
Reactor Vessel	SA 302 Gr. B LAS	26.7	50.0	44.15
Stabilizer Bracket	Inconel X-750	47.5(2)	---	92.3(2)
H8 Bracket	Inconel X-750	47.5(2)	---	92.3(2)
Tie Rod	316 SS	22.9(3)	---	15.6
Toggle Bolts	Inconel X-750	47.5(2)	---	92.3(2)
Upper Spring	Inconel X-750	47.5(2)	---	92.3(2)
Lower Spring	Inconel X-750	47.5(2)	---	92.3(2)
C-Spring	Inconel X-750	47.5(2)	---	92.3(2)
Upper Support	Inconel X-750	47.5(2)	---	92.3(2)
Shroud	304 SS	15.8	30.0	17.75

Notes:
(1) The NMP-1 FSAR shows an allowable stress value of 20.0 ksi for Inconel 600; however, this allowable was based on ASME Code, Section VIII, which is similar to current-day Section III, Class 2/3 allowables. Since the conical support was fabricated as part of the vessel, the Class 1 allowable of 23.3 ksi for Inconel 600 was used.
(2) Value taken from Reference 1.
(3) This allowable is based on material test reports, as determined using the methods of Appendix III of the ASME Code, Section III.

Table 2-5: Allowable Stress Limits

Stress Category	Normal/Upset Event Allowable	Emergency Event Allowable	Faulted Event Allowable
Primary Membrane (P_m)	S_m	$1.5S_m$	$2.0S_m$
Primary Membrane + Bending ($P_m + P_b$)	$1.5S_m$	$1.5*1.5S_m = 2.25S_m$	$2.0*1.5S_m = 3.0S_m$
Primary + Secondary ($P_m + P_b + Q$)	$3S_m$	No limits	No limits
Shear Stress	$0.6S_m$	$1.5*0.6S_m = 0.9S_m$	$2.0*0.6S_m = 1.2S_m$
Bearing Stress	$1.5S_y$	$1.5*1.5S_y = 2.25S_y$	$2.0*1.5S_y = 3.0S_y$

3.0 ANALYSIS AND RESULTS: CONICAL SUPPORT

Stress analysis was performed for the shroud conical support to fully evaluate all of the loads imposed as a result of anticipated reactor operation, as well as additional loads imposed on the conical support by the shroud repair hardware. The details of this stress evaluation are presented in this section, along with the results of the evaluation.

3.1 Finite Element Model

A detailed finite element model of the NMP-1 shroud conical support was developed using the ANSYS finite element computer program (Reference 2). Dimensions for the model were obtained from the Reference 3 drawings. The purpose of this model was to perform stress analysis of the conical support to fully evaluate all of the loading conditions specified in Reference 1 and detailed in Section 2.0. The model consisted of a 90° vessel/conical support segment composed of 7,764 three degree of freedom (DOF), isoparametric solid elements (STIF 45). The complete finite element model is shown in Figure 3-1.

The shroud support ring and the shroud were not included in the finite element model (i.e., the H8 weld was assumed to be completely failed). This condition leads to the most limiting conical support stresses since the conical support receives no additional support from the shroud support ring and shroud. The impact of the repair hardware on stresses in the H8 weld were assessed to further support this assumed condition, and was shown to have a negligible impact (see Appendix A).

A portion of the reactor vessel was included in the model so that the appropriate interaction at the conical support junction could be accounted for. The vessel ends were modeled far enough away (i.e., much farther than three attenuation lengths) from the junction so that end effects were insignificant. The repair hardware connection was placed in the center of the model (i.e., at 45°) so that edge effects from the 0° and 90° planes were insignificant in the region of interest.

A 90° segment (i.e., ¼ model) was utilized since the shroud repair consists of four nearly equally spaced tie rods. This model was also used to evaluate the six H8 weld repair brackets. Although the model effectively considered four of these brackets (since the model

was a ¼ model), the stress results demonstrated that the effects from one bracket do not influence the stresses at other bracket locations; therefore, the 90° model was deemed adequate for fully evaluating all loads imposed on the conical support by all of the shroud repair hardware and all vessel loads.

Symmetric boundary conditions were applied to the 0° and 90° edges of the model, and "roller" restraint was applied to the bottom of the model (i.e., radial motion allowed, no tangential motion allowed). The top of the vessel was coupled in the axial direction. A plot of the model with all applied boundary conditions is shown in Figure 3-2.

Stresses due to reactor pressure, lower shroud pressure drop (ΔP), thermal events, and all reactions from the shroud repair hardware were considered in this analysis.

Figure 3-1: NMP-1 Shroud Conical Support Finite Element Model

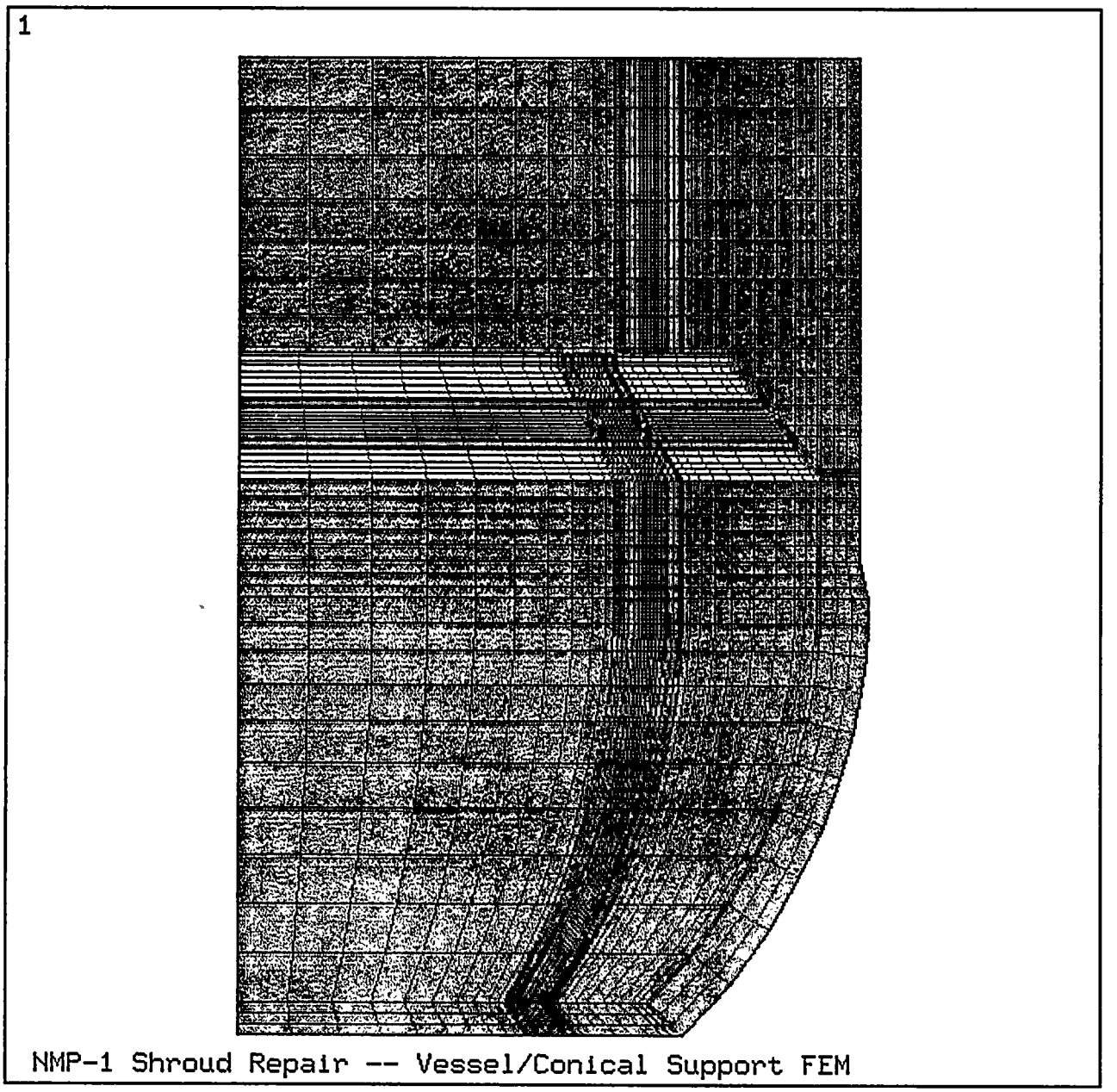

Figure 3-2: Boundary Conditions Applied to Finite Element Model

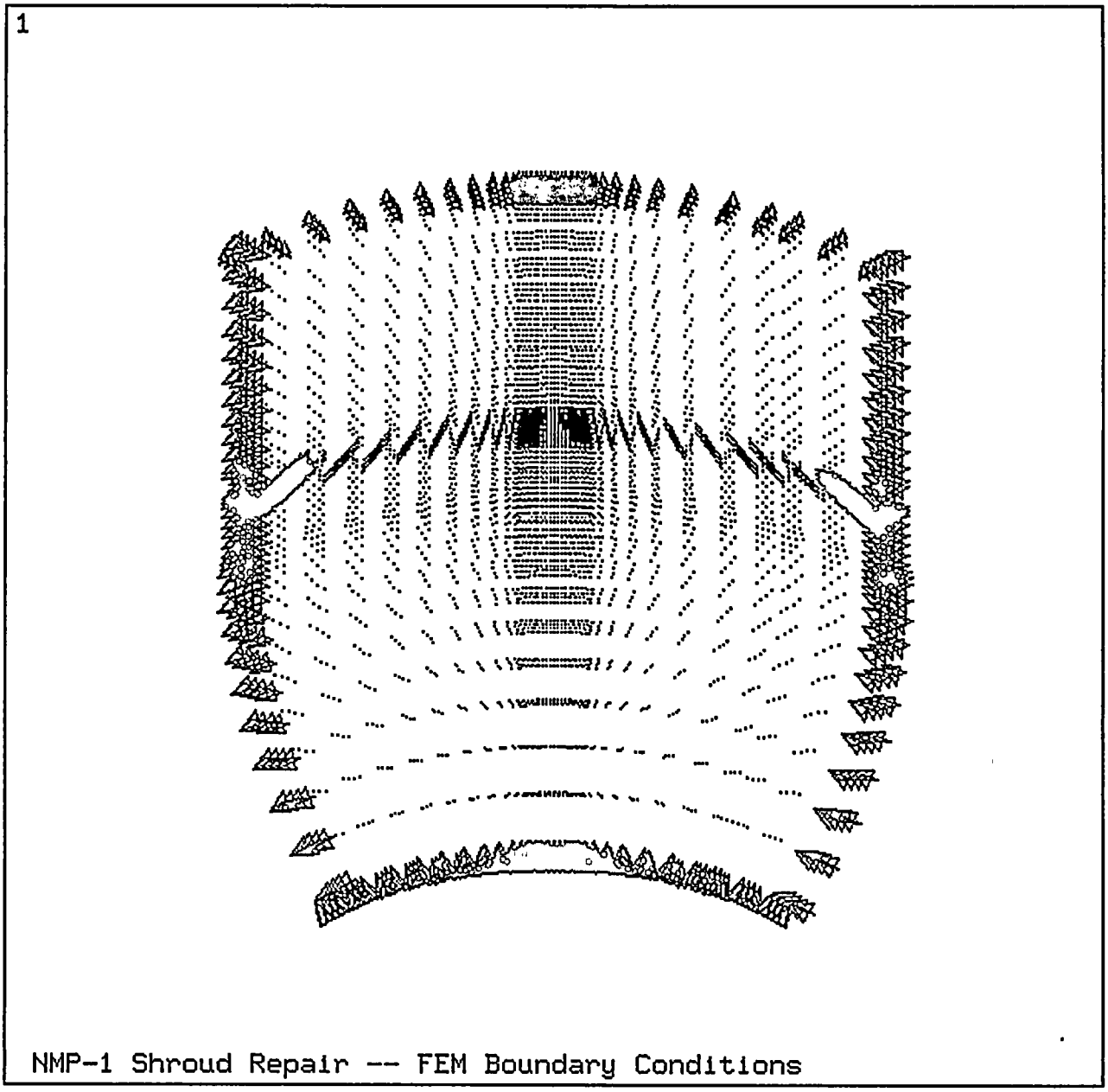

3.2 Applied Loads

Conical support loads were developed based on the operating condition definitions contained in Reference 1 and detailed in Section 2.0. These loads were applied to the finite element model created for the shroud conical support described in Section 3.1 in order to determine stresses. Nine (9) load cases were evaluated as shown in Table 2-2. The loads developed for application to the conical support are listed in Table 3-1 and are based on the values defined in Section 2.0. The finite element stress analysis details and results for the limiting load cases are provided in the sections which follow.

3.3 Stress Evaluation Methodology

Seven (7) unit loads applied to the conical support were separately analyzed: the five loads listed in Table 3-1, steady state thermal stresses at 535°F (maximum operating temperature per Reference 1) and thermal stresses resulting from the upset thermal event. Separate load cases were run for each of these unit loads so that they could be individually scaled and combined appropriately for each of the nine load combinations identified in Table 2-2. In addition, the separate unit load cases allowed for separation of primary and secondary stresses on the conical support for comparison to the appropriate allowable values. The classification of each unit load and the magnitude of load applied to the finite element model is shown in Table 3-2.

For the upset thermal event, a separate temperature solution was first performed for the model. For this separate case, bulk fluid temperatures and heat transfer coefficients were applied to the model as described in Table 3-3, and a steady state solution was obtained. The thermal stresses resulting from this event are considered conservative, since a steady state solution maximizes metal temperature gradients in the modeled structure.

The stress results from each of the seven unit loads were appropriately scaled and added together using the post processor utilities of the ANSYS computer program for all nine load combinations. Scaling factors used for this evaluation are given in Table 3-4, and are based on the ratio of the actual applied load for each condition divided by the unit load applied to the finite element model.

Table 3-2: Unit Loads Applied to Finite Element Model

No.	Unit Load Description	Load Classification[1]	Unit Load Applied to Model
1	Tie Rod Load	Primary	100,000 lb (vertical)
2	Reactor Pressure	Primary	1,000 psi
3	ΔP	Primary	10 psi
4	H8 Bracket Load[2]	Primary	128,016 lb (vertical)
5	Attachment Preload	Secondary	12,049 lb
6	Steady State Thermal	Secondary	545°F uniform temperature
7	Upset Thermal Event	Secondary	Steady state temperature solution based on boundary conditions described in Table 3-3

Notes: (1) The load classifications given here are in terms of the resulting linearized stresses on the conical support.

(2) The H8 bracket load consists of vertical loading as a result of deadweight and ΔP and, where applicable, seismic and asymmetric reaction loads due to the recirculation outlet break event.

Table 3-3: Boundary Conditions Used for Upset Thermal Run

Model Region	Bulk Fluid Temperature (°F)	Heat Transfer Coefficient (Btu/hr-ft^2-°F)
Outside of Reactor Vessel	100	0.2
Annulus (inside surface of vessel above conical support, top surface of conical support)	300	500
Lower plenum (inside surface of vessel below conical support, bottom surface of conical support)	545	500

Table 3-4: Scaling Factors Used in Stress Evaluation

Load Case	Stress Category	Scaling Factors[1,2]						
		Unit Load #1	Unit Load #2	Unit Load #3	Unit Load #4	Unit Load #5	Unit Load #6	Unit Load #7
Normal Operation	Primary	0.412	1.026	2.120	0.000	0.000	0.000	0.000
	Primary + Secondary	0.797	1.026	2.120	0.000	0.100	0.977	0.000
Upset #1	Primary	0.669	1.026	2.360	0.000	0.000	0.000	0.000
	Primary + Secondary	1.886	1.026	2.360	0.000	0.100	0.000	1.000
Upset #2	Primary	1.621	1.026	2.360	0.000	0.000	0.000	0.000
	Primary + Secondary	1.621	1.026	2.360	0.000	0.100	0.977	0.000
Emergency #1	Primary	1.621	1.026	2.120	0.000	0.000	0.000	0.000
Emergency #2	Primary	2.165	1.026	6.300	0.000	0.000	0.000	0.000
Emergency #3	Primary	0.534	1.026	-12.500	2.536	0.000	0.000	0.000
Faulted #1	Primary	3.117	1.026	6.300	0.000	0.000	0.000	0.000
Faulted #2	Primary	1.266	1.026	-12.500	3.085	0.000	0.000	0.000
Faulted #3	Primary	1.486	1.026	-12.500	3.272	0.000	0.000	0.000

Notes: (1) Scaling factor = Actual applied load (from Table 3-1) divided by the unit load applied to the finite element model (from Table 3-2).

(2) See Table 3-2 for a description of each unit load.

3.4 Stress Evaluation Results

The finite element stress results for each of the seven unit loads were scaled and added together for the twelve stress categories/load cases identified in Table 3-4. The resultant total stress profiles in the conical support were analyzed and compared to the appropriate allowable stress values identified in Table 2-5.

In order to obtain the appropriate stresses for comparison to allowable stress values, twelve sections were chosen throughout the conical support for stress linearization. These sections are identified in Figure 3-3 (for the region adjacent to the tie rod connection) and Figure 3-4 (for the region adjacent to the H8 bracket). These regions were chosen based on judgment considering regions of highest stress (as evidenced by the finite element model results) and enough cross sections to provide a complete over-all picture of the stress state in the conical support. The sections chosen also included the H9 weld attachment to the vessel as noted in Figures 3-3 and 3-4.

The stress linearization was performed for all sections using the ANSYS computer program post processing utilities for all stress categories/load cases. The limiting stress results for each stress category/load case are presented in Table 3-5. It is seen from these results that all stress allowables are maintained.

The stress results shown in Table 3-5 are also considered to be bounding for the vessel, since vessel stresses are equal to (or in most cases less than) the values shown in Table 3-5, and the vessel material is stronger than the conical support material (refer to S_m values in Table 2-5). In addition, the results shown in Table 3-5 also include weld H9 (conical support attachment weld to the vessel), which provides further support for this conclusion. Finally, the $P_m + P_b + Q$ stresses for the normal and upset load cases were also evaluated from a fatigue standpoint and were determined to have a negligible impact on fatigue usage, as shown in Table 3-6.

Figure 3-3: Stress Analysis Sections Near Tie Rod Attachment Location

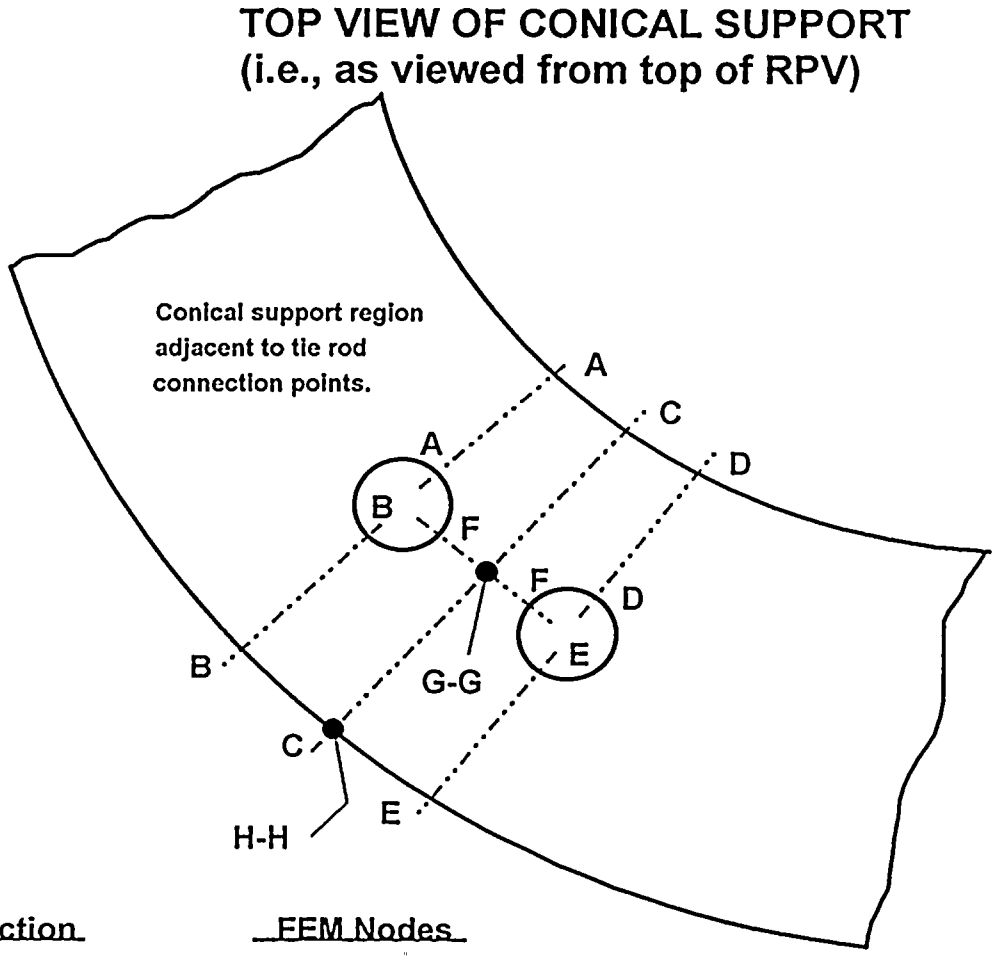

Section	FEM Nodes	
A-A	14016-14034	
B-B	14066-14103	
C-C	22016-22103	
D-D	30016-30034	
E-E	30066-30103	
F-F	17050-27050	
G-G *	22045-22046	
H-H *	22097-22098	(corresponds to weld H9)

* Sections G-G and H-H are oriented vertically down through conical support. All other sections are taken through conical support mid-section.

Figure 3-4: Stress Analysis Sections Near H8 Bracket Contact Location

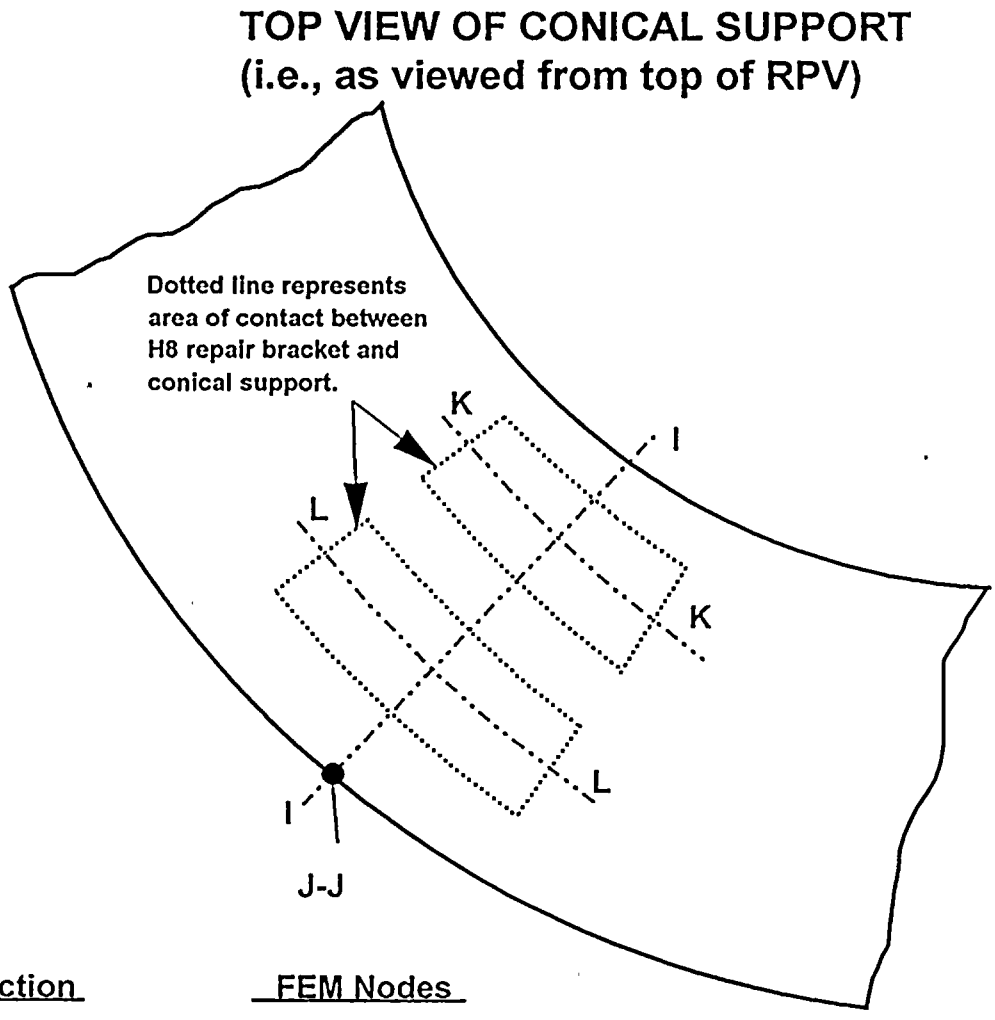

Section	FEM Nodes	
I-I	4016-4103	
J-J *	4097-4098	(corresponds to weld H9)
K-K	3009-5009	
L-L	3088-5088	

* Section J-J is oriented vertically down through conical support. All other sections are taken through conical support mid-section.

Table 3-6: Fatigue Evaluation for Normal and Upset Conditions

S_m = 23,300 psi E_a = 2.94E+07 psi
m = 1.7 E_c = 2.83E+07 psi
n = 0.3

Load Case	Limiting $P_m + P_b + Q$ Stress (psi)	Peak Stress (psi)	Total Stress (psi)	Stress Concentration Factor, K_t[1]	K_e	S_{alt}[2] (psi)	N_{allow}[3]	$N_{applied}$[4]	Fatigue Usage
NORMAL	18,650	15,670	34,320	4.00	1.00	43,446	70,863	120	0.0017
UPSET #1	39,650	1,150	40,800	4.00	1.00	76,886	4,787	30	0.0063
UPSET #2	30,210	24,860	55,070	1.00	1.00	26,505	1,224,020	120	0.0001

Notes: (1) Assumed to be 4.0 for weld at cone-to-vessel junction; 1.0 elsewhere.
(2) $S_{alt} = .1/2 * K_e * E_c/E_a * [(P_m+P_b+Q)K_t + Peak]$
(3) N_{allow} is obtained from Figure I-9.2.1 of Appendix I of Section III of the ASME Code.
(4) $N_{applied}$ is assumed to be 10 Loss of Feedwater Pump Events x 3 up/down temperature excursions per event = 30 cycles for upset #1, and is assumed to be 120 cycles for the Normal and Upset #2 events (corresponding to startup/shutdowns).

3.5 Evaluation of Shroud Conical Support Deformation

For the emergency and faulted load cases, secondary stresses are not limited per Reference 1. However, the FEM results from each of these load cases were reviewed to evaluate relative deformation of the shroud conical support. The relative deformations for the limiting emergency load case (Emergency #3) and the limiting faulted event (Faulted #3) are summarized in Table 3-7. These deflection values were evaluated with respect to their impact on the core spray lines attached to the shroud and found to be acceptable (see Appendix B).

4.0 ANALYSIS AND RESULTS: SHROUD AND TIE ROD ASSEMBLIES

Two detailed finite element models of the NMP-1 shroud and repair assembly were developed for stress analysis purposes to fully evaluate all of the loading conditions specified in Reference 1 for two different weld crack configurations. In model 1 the weld H8 is intact while in model 2 it is assumed cracked. For the latter case the shroud-support cone connection is insured by the installation of the of 6 support brackets. The model consisted of a 180° shroud segment composed of shell (modeled with solid elements), gaps (representing cracks), 3-D truss and spring elements. Repair spring and vertical tie rod assemblies were also included in this model as 3-D truss elements and lower brackets (for model 2 only) as 3-D beam elements simulating the repair hardware mechanical characteristics. A 180° segment was necessitated by the need to evaluate the non-axisymmetric loads.

The shroud spring and vertical tie rod components were separately modeled in detail to evaluate their mechanical characteristics and stresses. These models are described in detail below.

These assemblies were modeled in detail using the COSMOS finite element code. COSMOS/M is a PC based finite element analysis computer code. The code is developed by Structural Research and Analysis Corporation (SRAC) of Los Angeles California. It has been verified for use in the nuclear power industry per the requirements of 10CFR50 Appendix B and the applicable sections of ANSI/ASME QA-1 and related supplements. Per contractual obligations, SRAC transmits "bug-reports" to GE whenever there are deficiencies discovered for resolution.

The COSMOS/M user guide shows a close comparison between finite element analysis results and closed form solution for over 1000 problems of different types elements and loading conditions. For validating COSMOS/M for NMP-1 shroud analysis application, the verification problems for the elements used in the shroud analysis (Solids, 3D beam, rigid bar, spring, coupling and gap) were reanalyzed using version 1.70 of COSMOS/M. The results of the analysis are in good comparison of the closed form solutions.

Also separate models of springs were made to assess their mechanical characteristics used in the global models 1 & 2 and their stress distribution.

4.1 Shroud Upper Spring Finite Element Model

The shroud upper spring consists of a beam-like structure on two simple supports. To evaluate the accurate linear spring constant and stress values, a finite element model was made with solid elements. Figure 4-1 depicts the meshing of this spring. The model is assumed hinged at the support locations and under a figurative perpendicular load of 30,000 lbs at the location of connection to the shroud. Figures 4-2 and 4-3 show the distribution of Von Mises stress and displacements perpendicular to the beam. The upper spring's linear spring constant extracted from the detailed model is used in the global model to represent the spring. To calculate the proper actual maximum stresses, the maximum stresses extracted from this model are prorated with actual loads extracted from the global model.

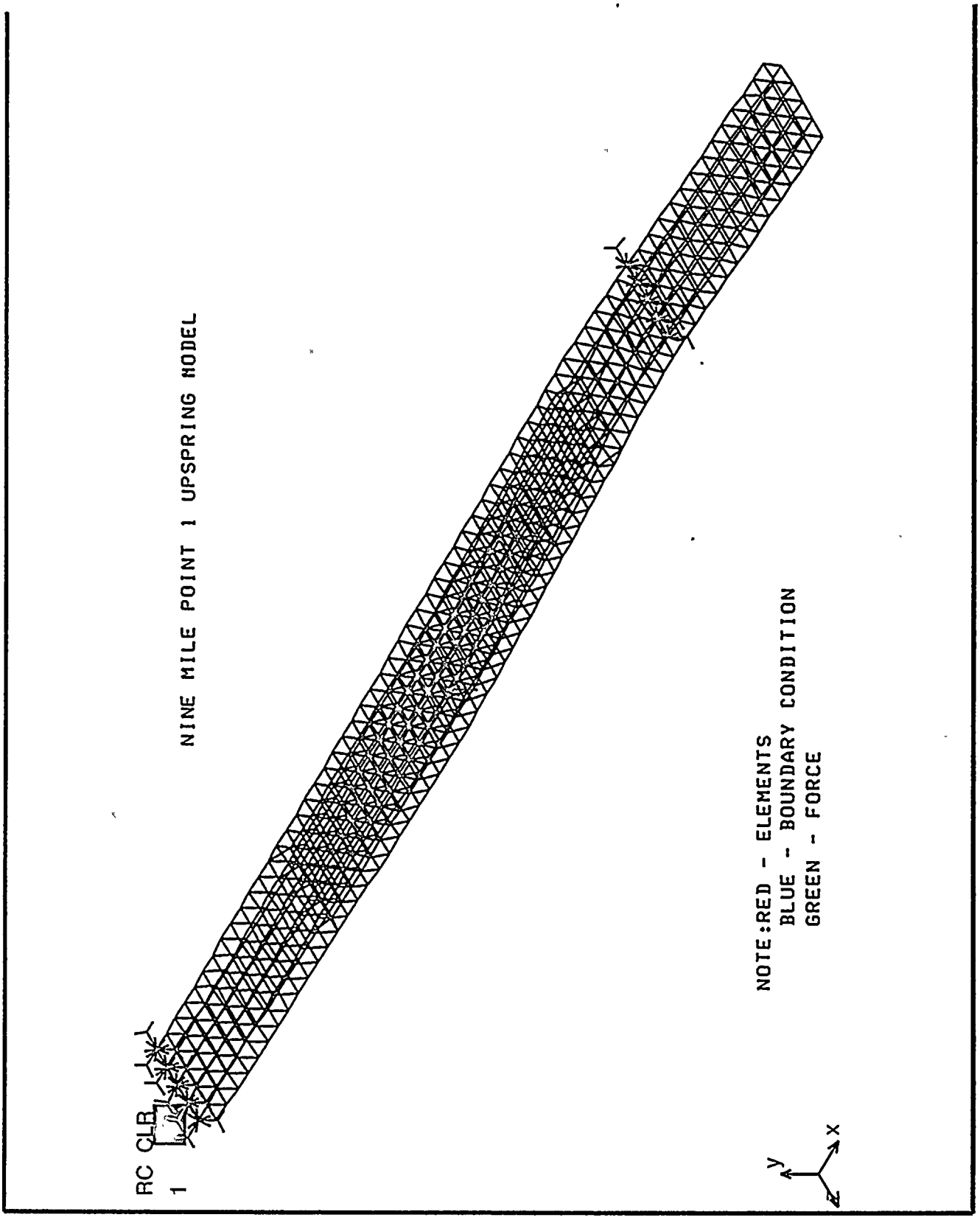

Figure 4-1: Shroud Upper Spring Finite Element Model

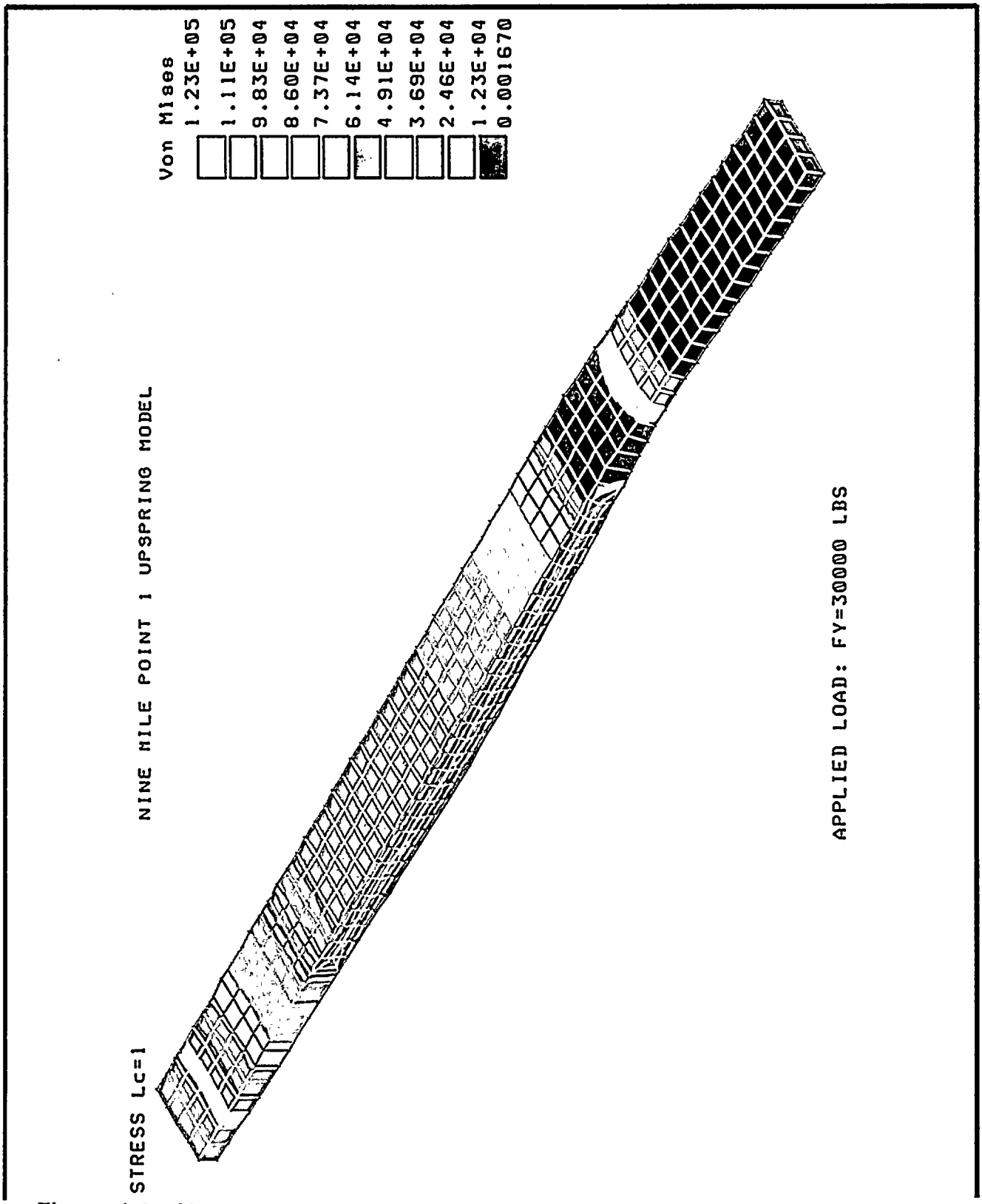

Figure 4-2: Shroud Upper Spring Von Mises Stress Distribution Due to a Figurative Load of 30,000 lb.

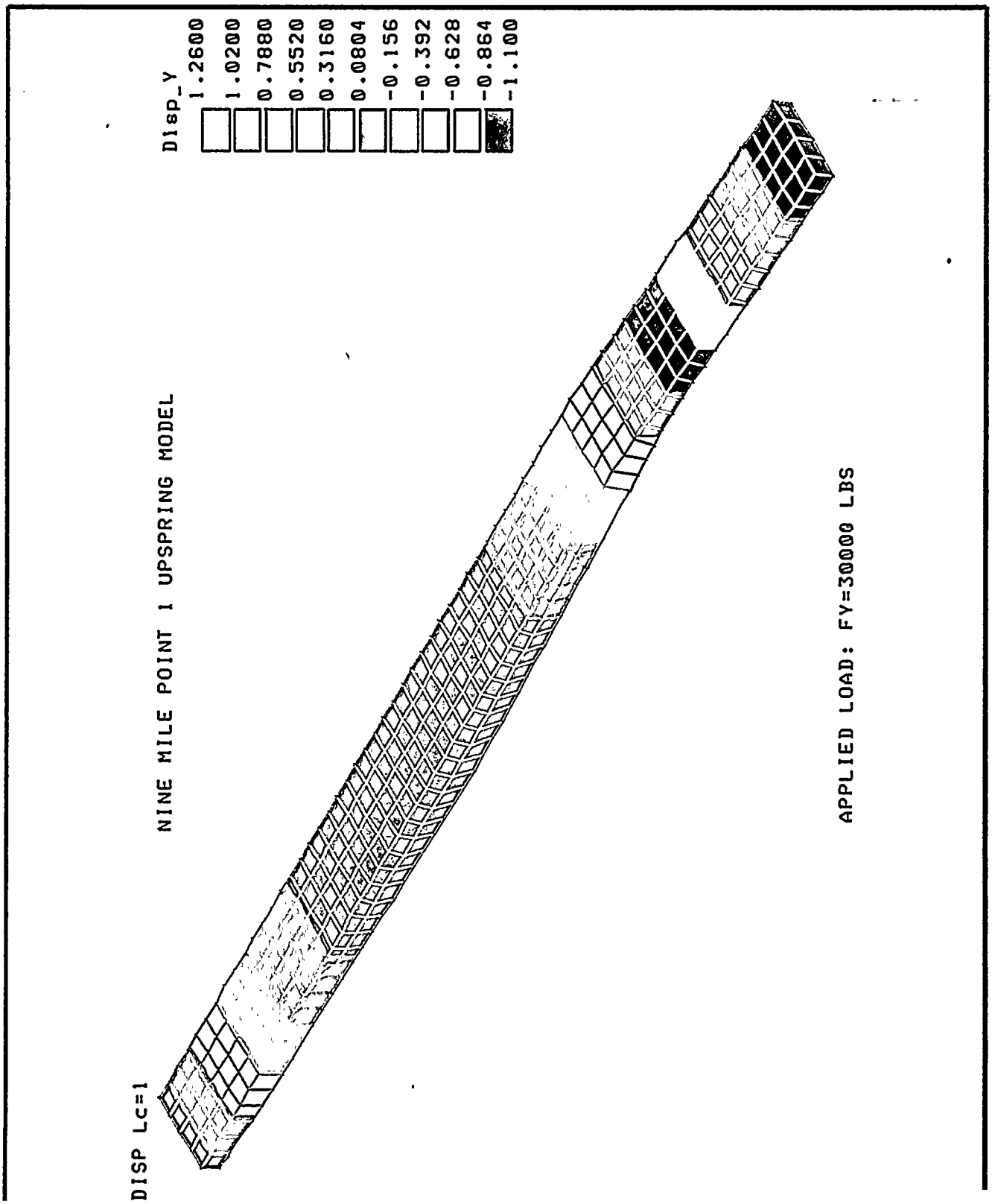

Figure 4-3: Shroud Upper Spring Displacement (Perpendicular to the Axis of Spring) Distribution Due to a Figurative Load of 30,000 lb.

4.2 Shroud Lower Spring Finite Element Model

The shroud lower spring consists of a diapason-like structure with the fork handle on a simple support, one branch hinged at the location of connection with the vessel and the other branch under the load representing the transmitted shroud side load at its point of connection. To evaluate the accurate linear spring constant and stress values, a finite element model was made with solid elements. Figure 4-4 depicts the meshing of this spring. The model is assumed hinged at the support locations and under a figurative perpendicular load of 80,000 lbs at the location of contact with the shroud. Figures 4-5 and 4-6 show the distribution of Von Mises stress and displacements perpendicular to the beam, respectively. The lower spring's linear spring constant, extracted from the detailed model, is used in the global model to represent this spring. To calculate the proper actual maximum stresses, the maximum stresses extracted from this model are prorated with actual loads extracted from the global model.

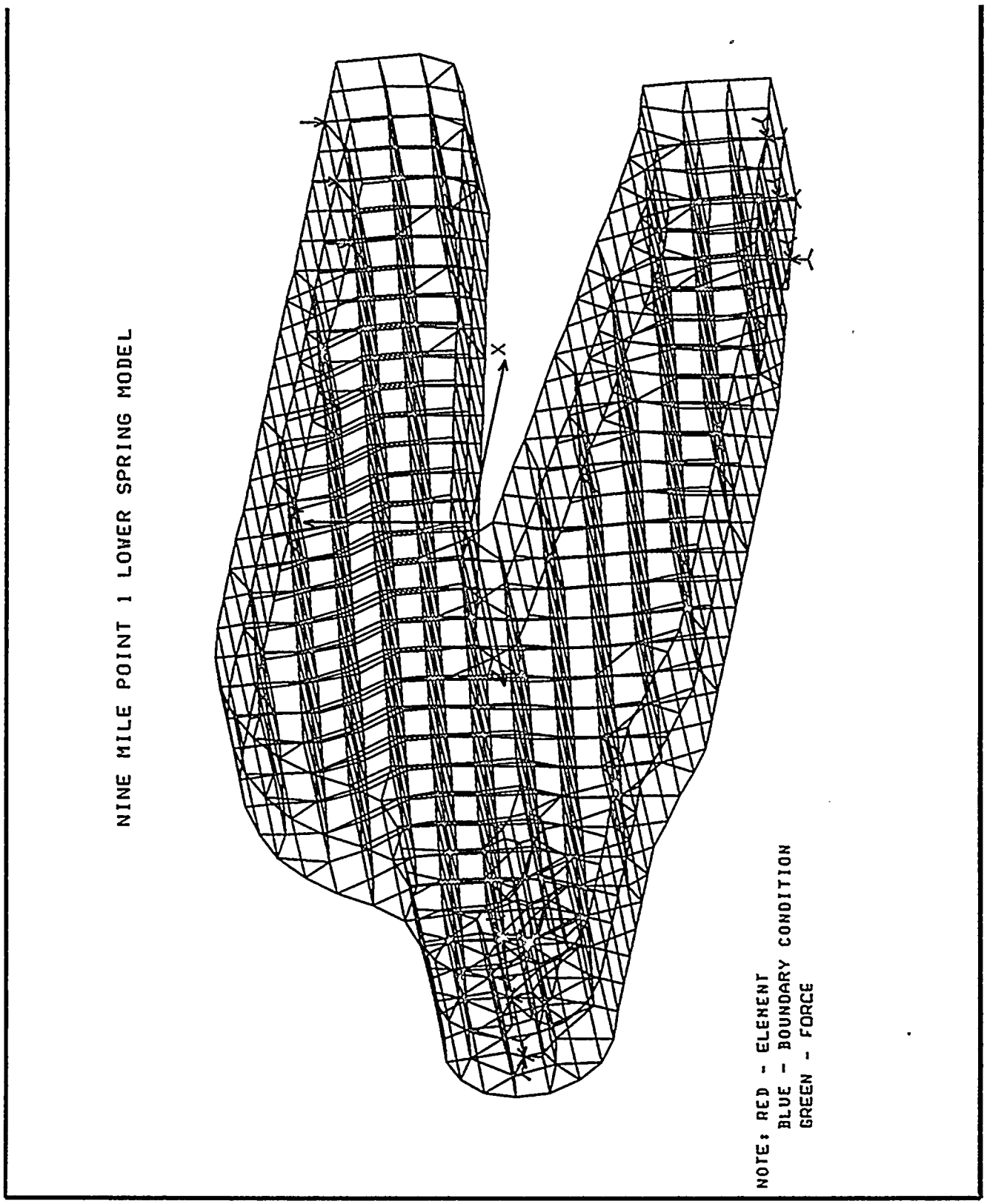

Figure 4-4: Shroud Lower Spring Finite Element Model

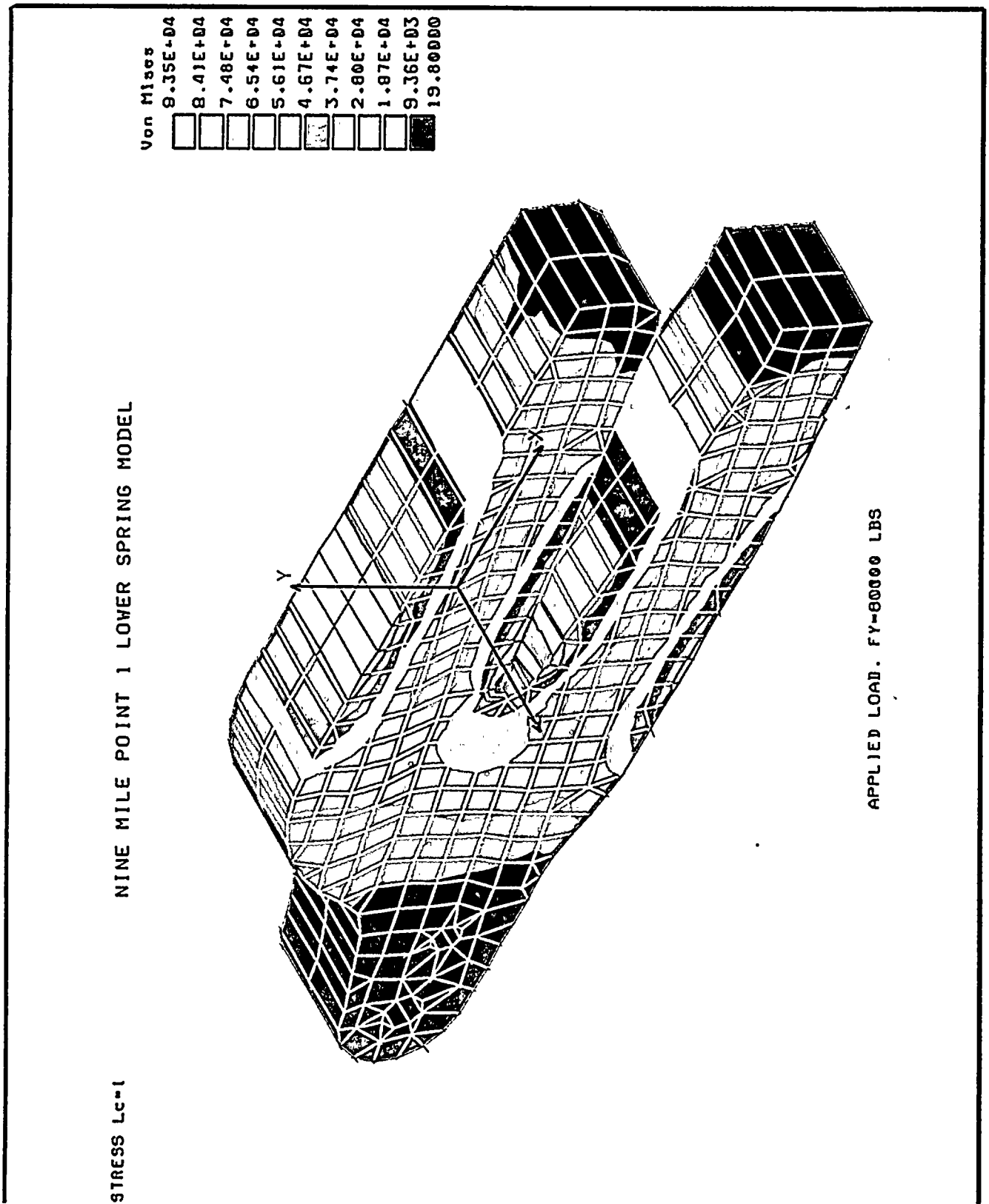

Figure 4-5: Shroud Lower Spring Von Mises Stress Distribution Due to a Figurative Load of 80,000 lb.

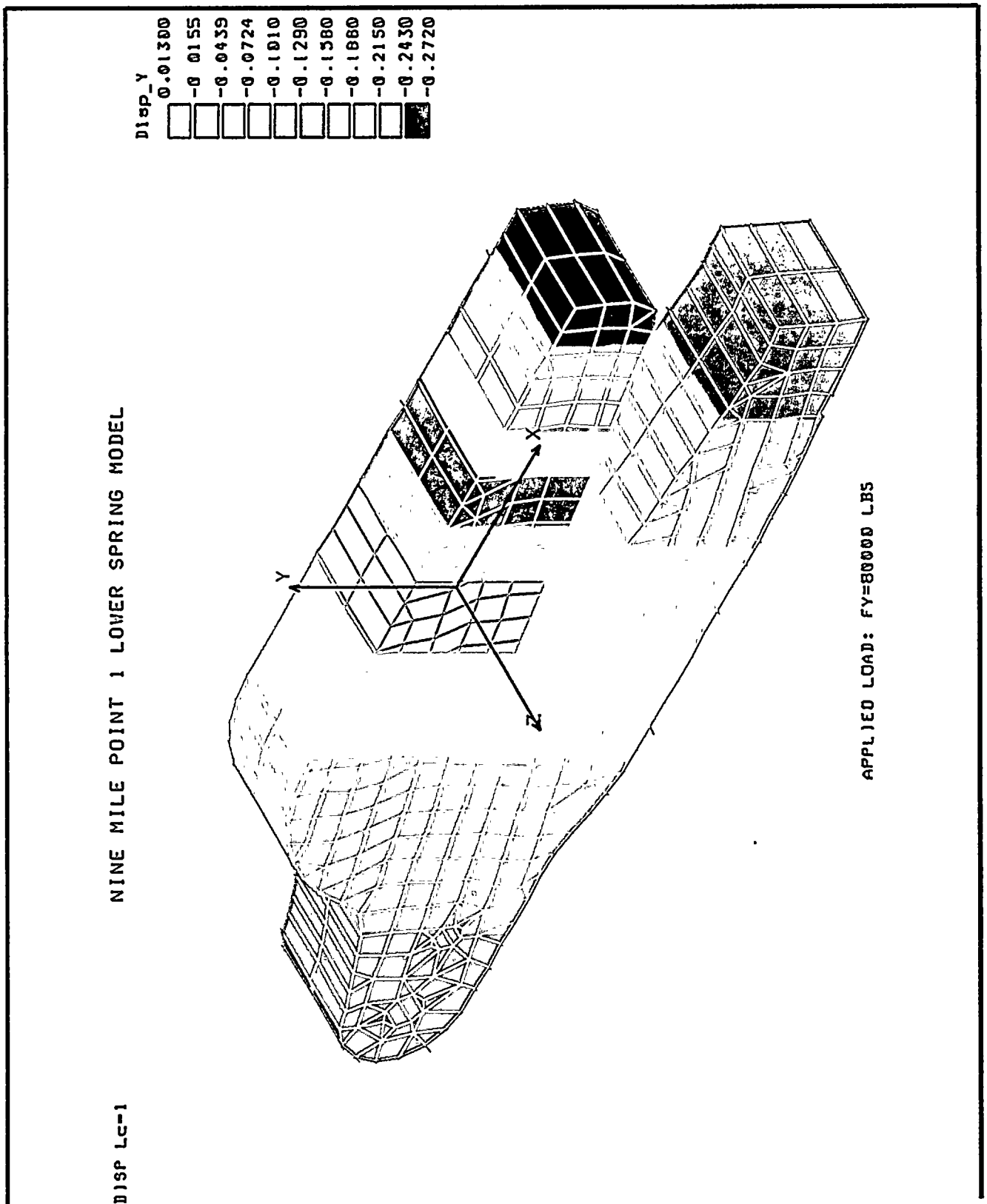

Figure 4-6: Shroud Lower Spring Displacement Distribution Due to a Figurative Load of 80,000 lb.

4.3 Tie Rod Upper Support Finite Element Model

The tie rod upper support used to tie up the shroud consists of a complex shape structure. The upper part of the structure hangs on the steam dam and rests on the shroud flange. The tie rod is connected to the lower part of this support. To evaluate the accurate linear spring constant and stress values, a finite element model was made with solid elements. Figure 4-7 depicts the meshing of this support. The model is assumed fixed at its seat on the shroud flange and hinged at the shroud connection. This model is subjected to an arbitrary load of 137,000 lbs, at the proper location to represent the tie rod force. Figures 4-8 and 4-9 show the distribution of Von Mises stress and global displacement for vertical loading, respectively. The lower spring's linear spring constant extracted from the detailed model is used in the global model to represent this spring. To calculate the proper actual maximum stresses, the maximum stresses extracted from this model are prorated with actual loads extracted from the global model.

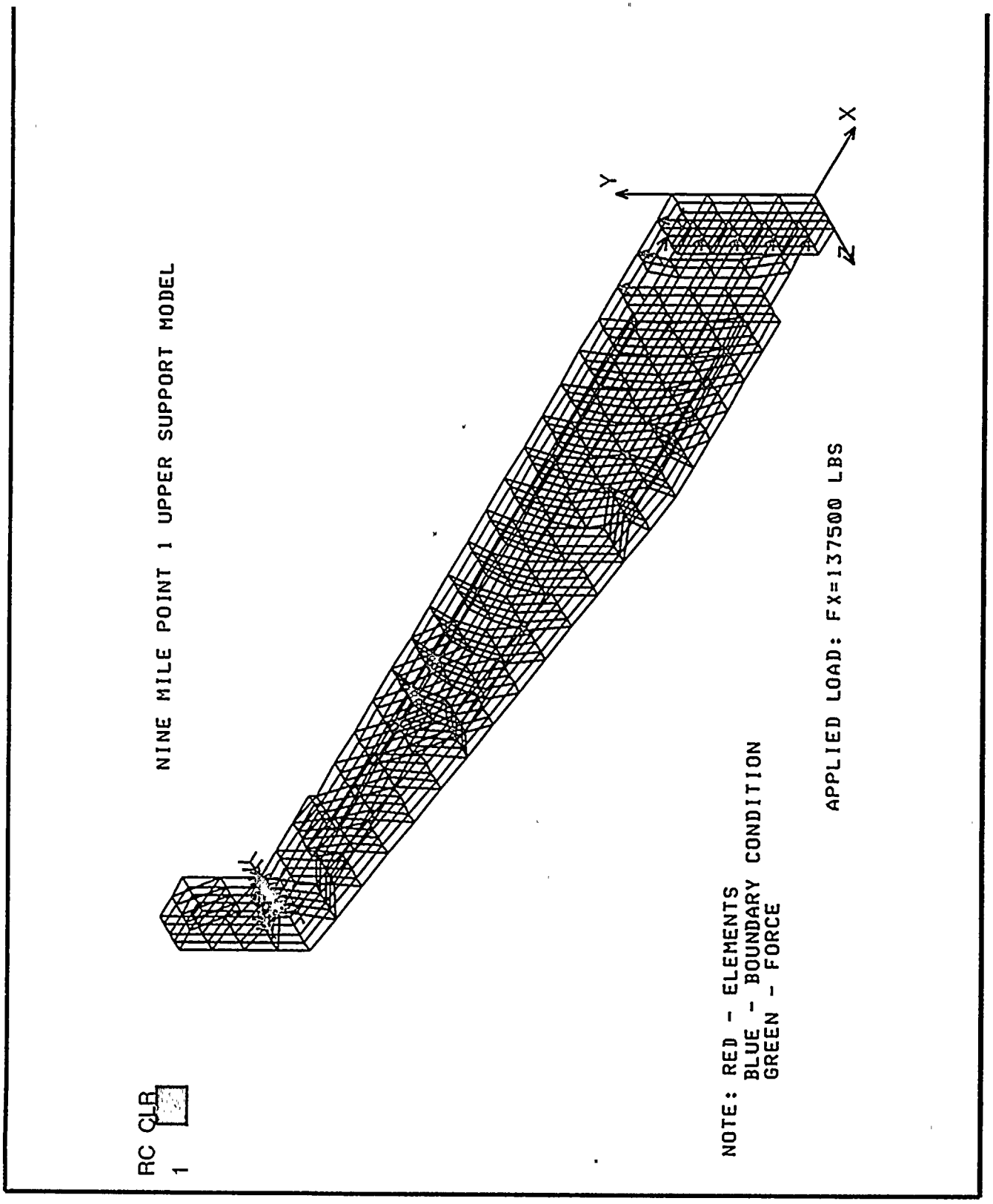

Figure 4-7: Tie Rod Upper Support Finite Element Model

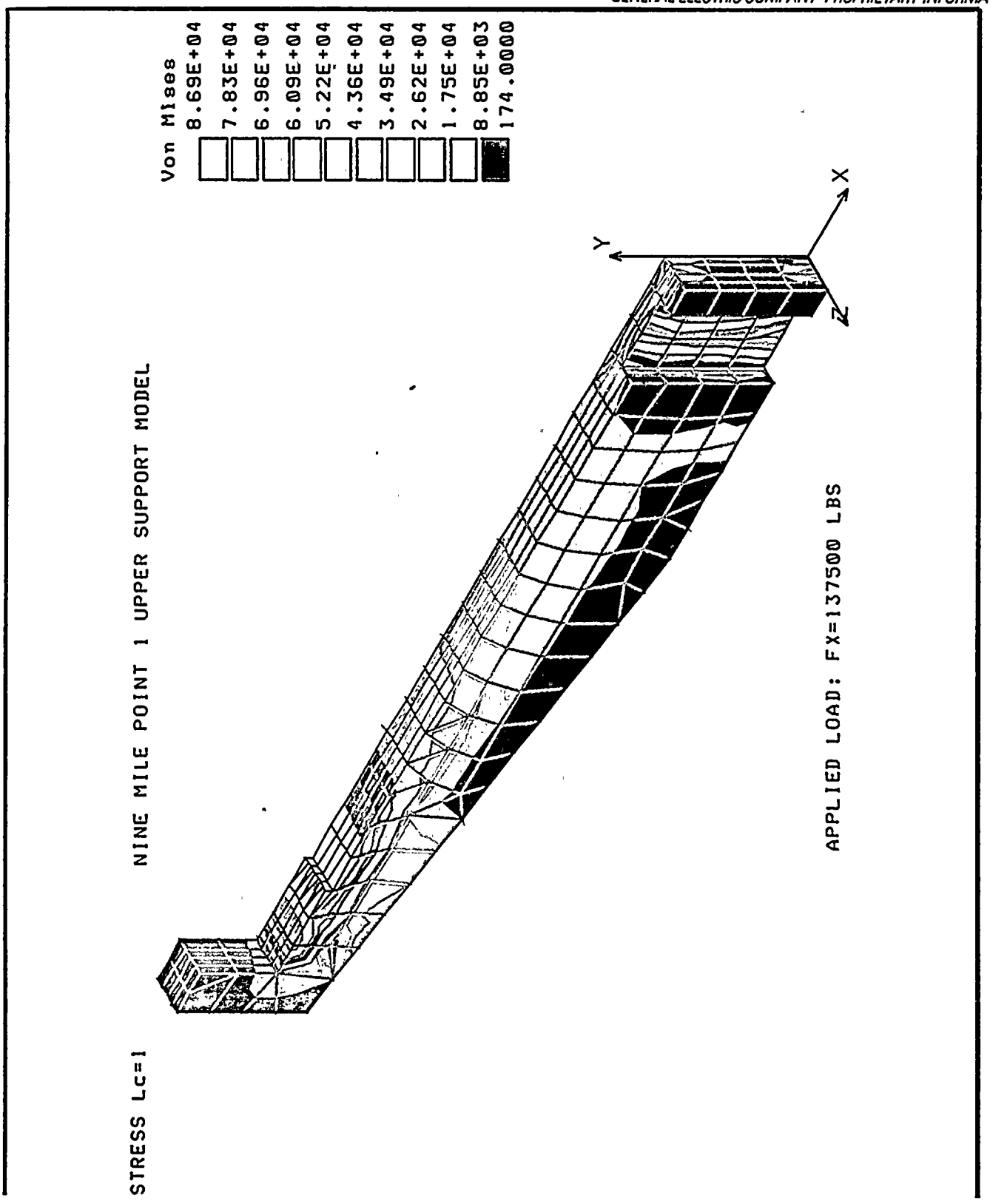

Figure 4-8: Tie Rod Upper Support Von Mises Stress Distribution Due to a Figurative Vertical Load of 137,500 lb.

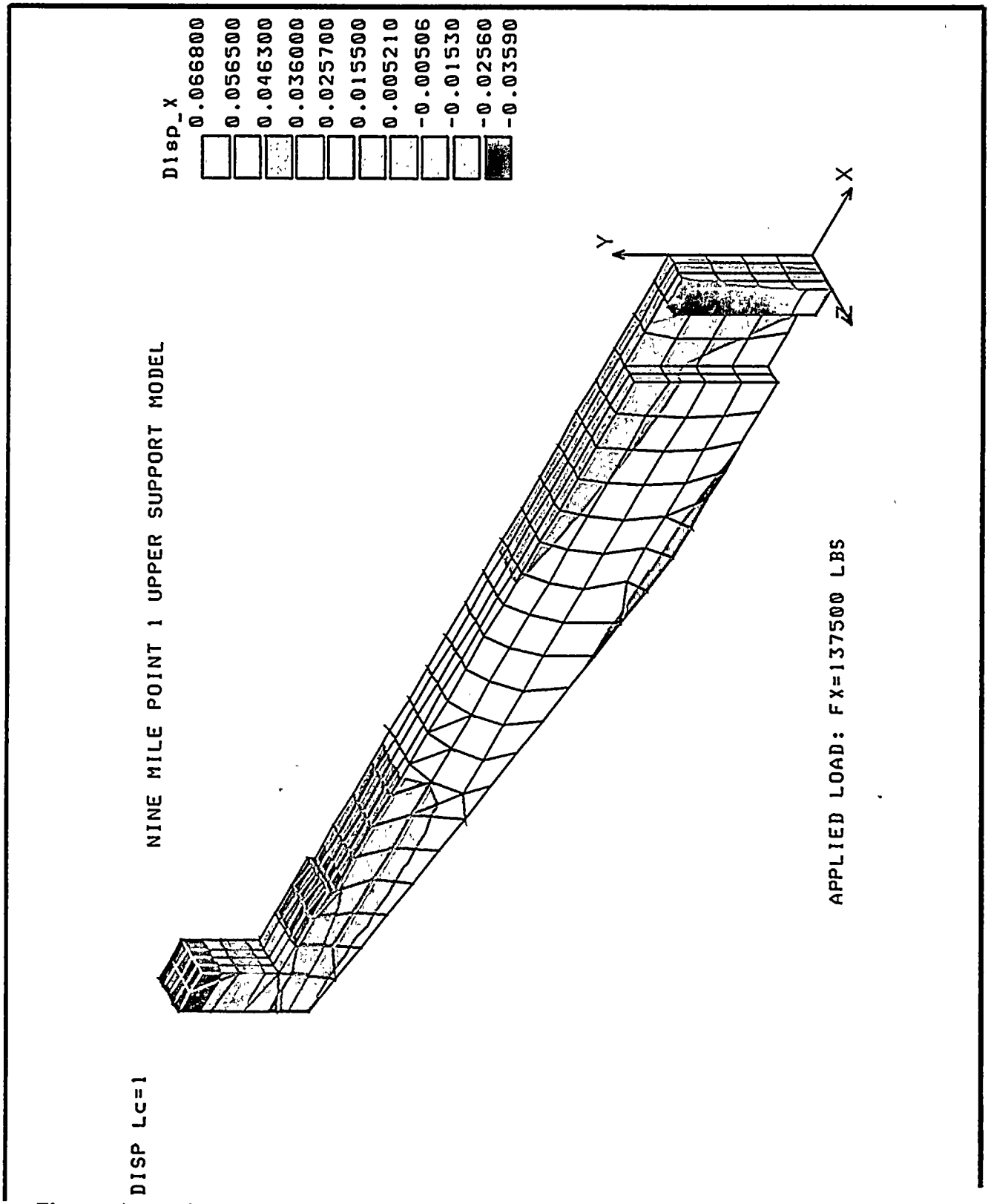

Figure 4-9: Tie Rod Upper Support Global Displacement Due to a Figurative Vertical Load of 137,500 lb.

4.4 Tie Rod C-Spring Finite Element Model

The tie rod C-spring used to tie down the shroud consists of a C-shaped structure. To evaluate the accurate linear spring constant and stress values, a finite element model was made with solid elements. Figure 4-10 depicts the meshing of this spring. The model is assumed hinged at the top connection to the tie rod and under an arbitrary downward load of 275,000 lbs on its bottom connection to the toggle bolts. Figures 4-11 and 4-12 show the distribution of Von Mises stresses and the global displacement in this spring, respectively. The C-spring's linear spring constant extracted from the detailed model is used in the global model to represent this spring. To calculate the proper actual maximum stresses, the maximum stresses extracted from this model are prorated with actual loads extracted from the global model.

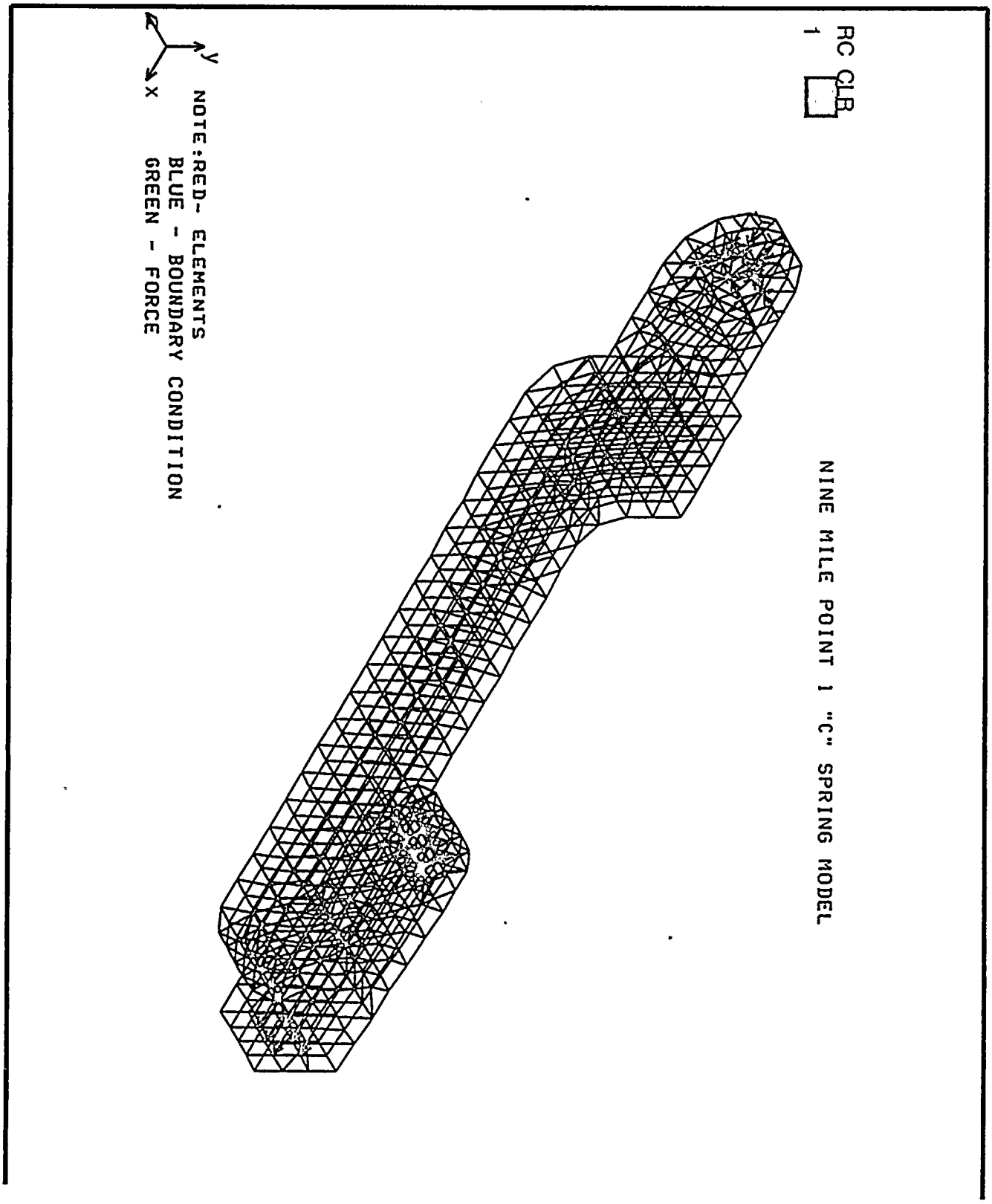

Figure 4-10: Tie Rod C-Spring Finite Element Model

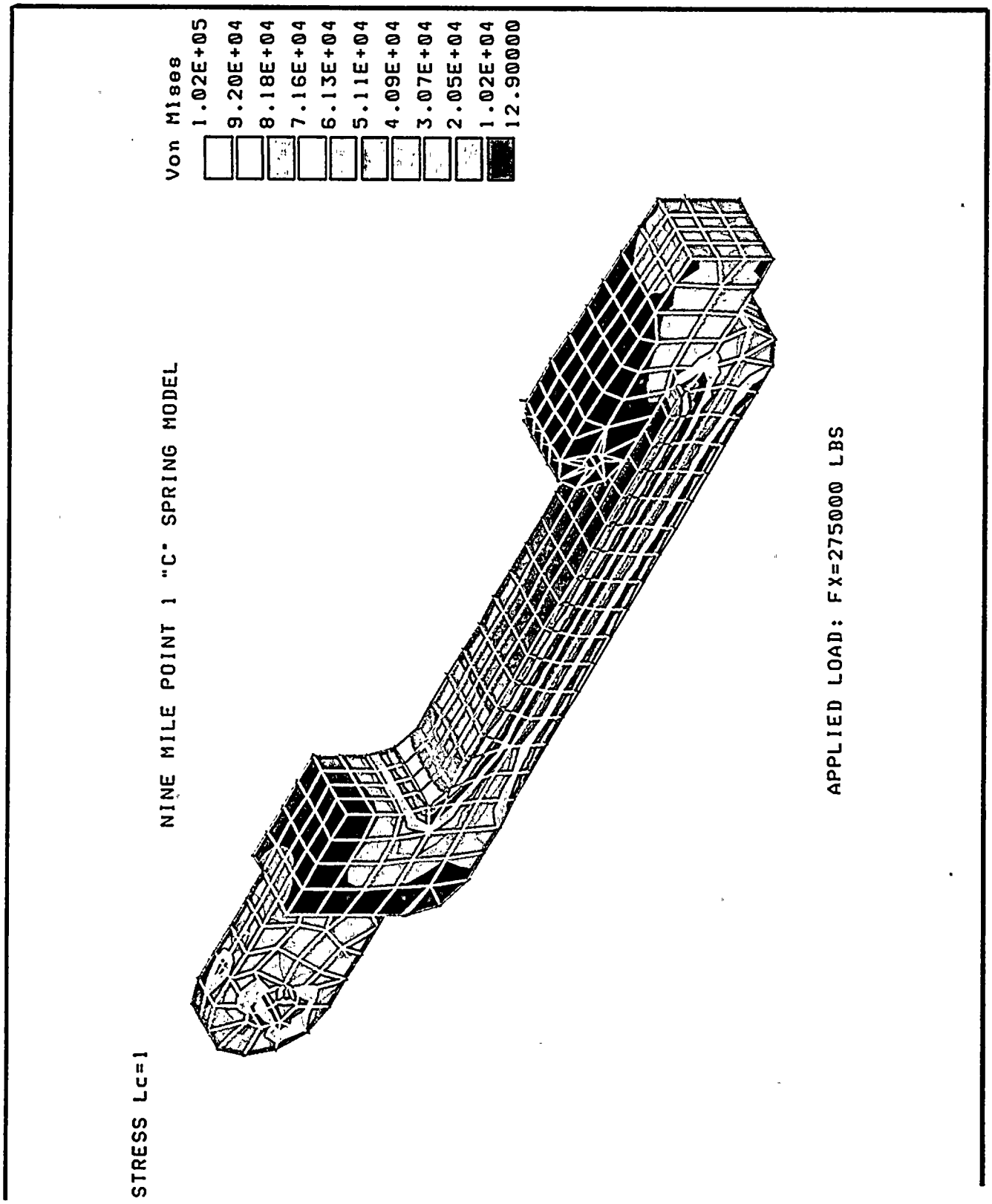

Figure 4-11: Tie Rod C-Spring Von Mises Stress Distribution Due to a Figurative Vertical Load of 275,000 lb.

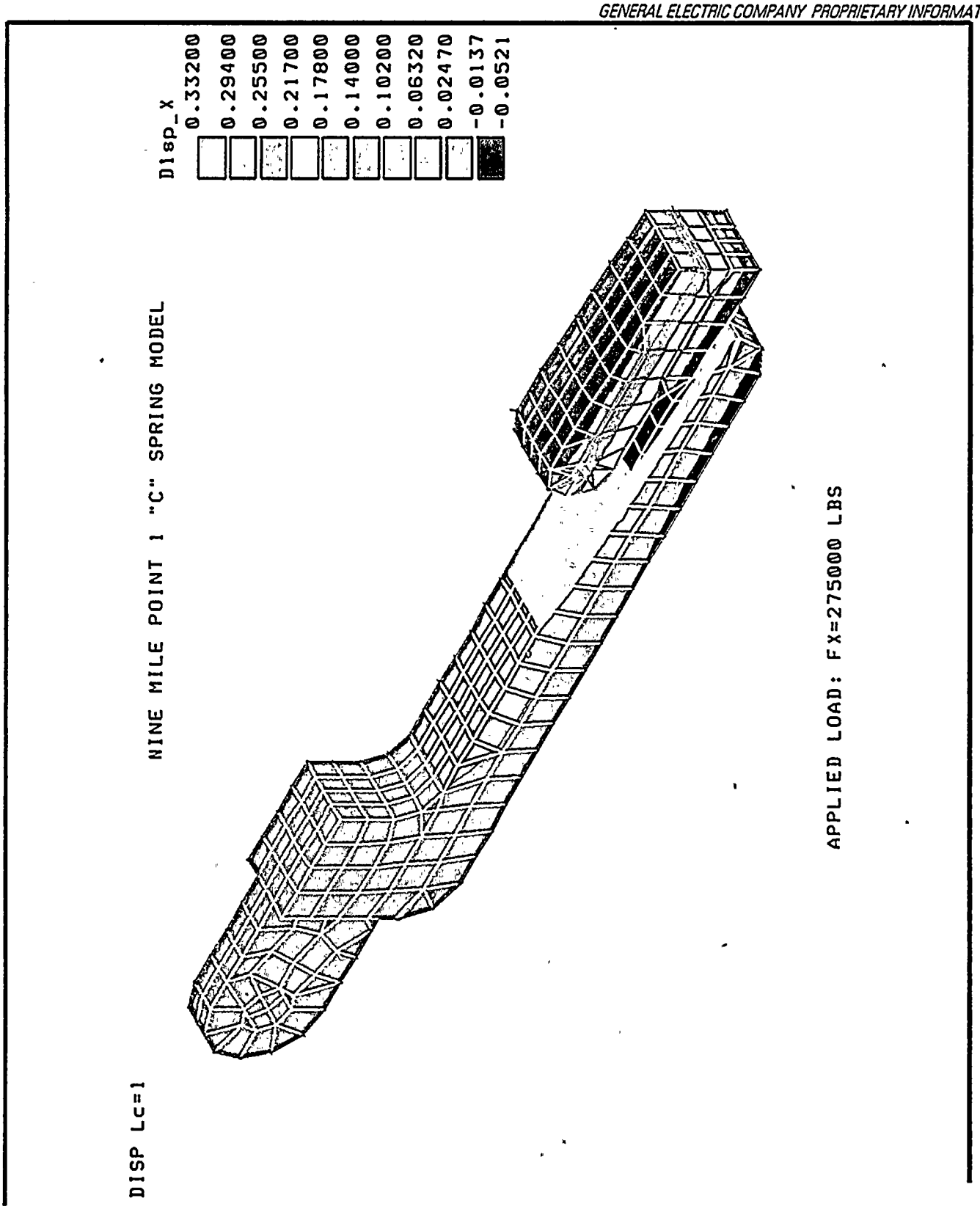

Figure 4-12: Tie Rod C-Spring Longitudinal Displacement Due to a Figurative Vertical Load of 275,000 lb.

4.5 Shroud 180° Shell Finite Element Models

Two global shroud models were made to represent one case with the H8 weld intact and another case with the H8 weld cracked. The two models are intended to represent the different critical combinations of horizontal weld cracks. Note that the angles given here are in reference to the finite element model and may be different from angles specified on drawings.

4.5.1 MODEL 1: H2-H6A-H7 CRACKED AND H8 INTACT

This model represents the shroud with welds H2, H6A and H7 cracked while H8 is intact. These cracks are judged sufficient to represent all horizontal welds up to H7 cracked in the finite element analysis. Since H8 is assumed intact, the support ring is included in the model. In this case the connection between the shroud and support cone is insured by H8 weld. The following explains the modeling details.

4.5.1.1 The 180° shroud upper ring was represented by solid elements.

4.5.1.2 The 180° upper shroud cylinder was represented by solid elements.

4.5.1.3 The 180° top guide ring was represented by solid elements.

4.5.1.4 The 180° mid shroud shell was represented by solid elements.

4.5.1.5 The 180° core support plate ring was represented by solid elements.

4.5.1.6 The 180° lower shroud cylinder was represented by solid elements.

4.5.1.7 The 180° shroud support cone was represented by solid elements.

4.5.1.8 The upper shroud spring at 90° was represented by a truss element having the stiffness extracted from the detailed finite element analysis explained in Section 4.1. The vessel side end of the element was fixed and the opposite end was connected to the top guide support ring to limit the horizontal motion.

4.5.1.9 The upper shroud springs at 0° and 180° were represented by truss elements having 1/2 the stiffness extracted from the detailed finite element analysis, as explained in Section 4.1. The use of a 1/2 multiplier was to accommodate the half-symmetry at the 0° and 180° planes. The vessel end of the elements were fixed and the opposite ends were connected to the top guide support ring to limit the horizontal motion.

4.5.1.10 The lower shroud spring at 90° was represented by a truss element having the stiffness extracted from the detailed finite element analysis explained in Section 4.2.

4.5.1.11 The lower shroud spring at 0° and 180° were represented by a truss element having 1/2 the stiffness extracted from the detailed finite element analysis, as explained in Section 4.2. The use of a 1/2 multiplier was to accommodate the half-symmetry at the 0° and 180° planes. The vessel end of the element was fixed and the opposite end was connected to the top guide support ring to limit the horizontal motion

4.5.1.12 The tie rod assembly at 90° was represented by a truss element having the stiffness extracted from both the detailed finite element analysis explained in Sections 4.3 and 4.4 and connecting rod characteristic hand calculations.

4.5.1.13 The tie rod assemblies at 0° and 180° were represented by truss elements, each having a stiffness equal to 1/2 of the stiffness extracted from the detailed finite element analysis, explained in Sections 4.3 and 4.4, and connecting rod characteristic hand calculations. The use of a 1/2 multiplier was to accommodate the half-symmetry at the 0° and 180° planes.

4.5.1.14 Welds H2, H6A and H7 were modeled as entirely cracked. This was judged to be the most representative for all horizontal weld cracking up to H7 in the finite element model to have an accurate account of the side motions of the shroud. The cracks were modeled using gap elements which transmit vertical compression force only when the gaps are closed. It was assumed that the gap nodes are linked for horizontal motion. To eliminate indeterminate vertical displacements of gaps that are in series, small springs were included between the gap ends. These springs allowed a reasonable distribution of the vertical displacements between the H2, H6A and H7 gaps. The vertical displacements are the result of the extension of the

tie rod due to the upward pressure forces, upward seismic forces or temperature effects.

4.5.1.15 The shroud support ring was represented by solid elements. The appropriate nodes of these elements were coupled to the appropriate support cone element nodes. This coupling insures H8 weld connection.

4.5.2 MODEL 2: H2-H6A-H7-H8 CRACKED

This model represents the shroud with welds H2, H6A, H7 and H8 cracked. These cracks are judged sufficient to represent all horizontal welds cracked in the finite element analysis. Since H7 and H8 are assumed cracked, no support ring is included in this model. The connection between the shroud and the support cone is ensured by support brackets. The following explains the modeling details.

4.5.2.1 The 180° shroud upper ring was represented by solid elements.

4.5.2.2 The 180° upper shroud cylinder was represented by solid elements.

4.5.2.3 The 180° top guide ring was represented by solid elements.

4.5.2.4 The 180° mid shroud shell was represented by solid elements.

4.5.2.5 The 180° lower shroud cylinder was represented by solid elements.

4.5.2.6 The 180° shroud support cone was represented by solid elements.

4.5.2.7 The upper shroud spring at 90° was represented by a truss element having the stiffness extracted from the detailed finite element analysis explained in Section 4.1. The vessel end of the element was fixed and the opposite end was connected to the top guide support ring to limit the horizontal motion.

4.5.2.8 The upper shroud springs at 0° and 180° were represented by truss elements having 1/2 the stiffness extracted from a detailed finite element analysis, as explained in

Section 4.1. The use of a 1/2 multiplier was to accommodate the half-symmetry at the 0° and 180° planes. The vessel end of the elements were fixed and the opposite ends were connected to the top guide support ring to limit the horizontal motion.

4.5.2.9 The lower shroud spring at 90° was represented by a truss element having the stiffness extracted from the detailed finite element analysis explained in Section 4.2.

4.5.2.10 The lower shroud spring at 0° and 180° were represented by a truss element having 1/2 the stiffness extracted from the detailed finite element analysis, as explained in Section 4.2. The use of a 1/2 multiplier was to accommodate the half-symmetry at the 0° and 180° planes. The vessel end of the element was fixed and the opposite end was connected to the top guide support ring to limit the horizontal motion

4.5.2.11 The tie rod assembly at 90° was represented by a truss element having the stiffness extracted from both the detailed finite element analysis explained in Sections 4.3 and 4.4 and connecting rod characteristic hand calculations.

4.5.2.12 The tie rod assemblies at 0° and 180° were represented by truss elements, each having a stiffness equal to 1/2 of the stiffness extracted from the detailed finite element analysis, as explained in Sections 4.3 and 4.4, and connecting rod characteristic hand calculations. The use of a 1/2 multiplier was to accommodate the half-symmetry at the 0° and 180° planes.

4.5.2.13 Welds H2, H6A, H7 and H8 were modeled as entirely cracked. This was judged to be the most representative for all horizontal weld cracking up to H8 in the finite element model to have an accurate account of the side motions of the shroud. The cracks were modeled using gap elements which transmit vertical compression force only when the gaps are closed. It was assumed that the gap nodes are linked for horizontal motion. To eliminate indeterminate vertical displacements of gaps that are in series, small springs were included between the gap ends. These springs allowed a reasonable distribution of the vertical displacements between the H2, H6A and H7 gaps. The vertical displacements are the result of the extension of the tie rod due to the upward pressure forces, upward seismic forces or temperature effects.

4.5.2.14 The shroud support brackets at 30°, 90° and 120° were represented by 3D-beam elements. The location angles for the brackets used in the model were selected to conserve the symmetry of the model. Therefore, these angles differ from the actual locations slightly. However, this approximation was considered appropriate by engineering judgment. The upper ends of the brackets were firmly connected to the shroud using horizontal and vertical 3D-beam elements; this was necessary in order to match the degrees of freedom of the 3D-beam and solid elements. The lower ends of the brackets were connected to the appropriate locations on the shroud support cone by means of gap elements.

4.6 Load Combination

The different load cases are summarized in Table 2-2. Examination of the loading in Table 2-2 reveals that the most limiting cases are 1, 3, 5, 7 and 8 for the repair hardware and shroud. For shroud evaluation, the case 2 is also considered. There is a small horizontal load that exists in the asymmetric loading related to the suction recirculation line break. However, the effect of this horizontal load is judged to be negligible for shroud stress analysis. It should be noted that in the seismic analysis (Reference 6) many cases were considered. These cases are related to various weld failure assumptions and eventual combination of failures in different welds. For the purposes of conservatism, the bounding results from these analyses are used in the evaluation of the above load combinations. The conservative nature of this method is based on the fact that the envelope of each effect (force) is selected knowing that the maximums are occurring at different times.

The different finite element models are subjected to the selected loadings. The material properties of the different components based on the ASME Code at 550°F are summarized in Table 2-3. The allowable stress values used for stress evaluation, are defined in Table 2-4 and the allowable stress limits are defined in Table 2-5.

4.7 Shroud Upper Spring Stress Evaluation

To evaluate the accurate linear spring constant and stress values, a finite element model was made with solid elements, as shown in Figure 4-1. The model is assumed hinged

at the support locations and under a figurative perpendicular load of 30,000 lbs at the location of connection to the shroud. Figure 4-13 shows the distribution of principal stress in the upper spring.

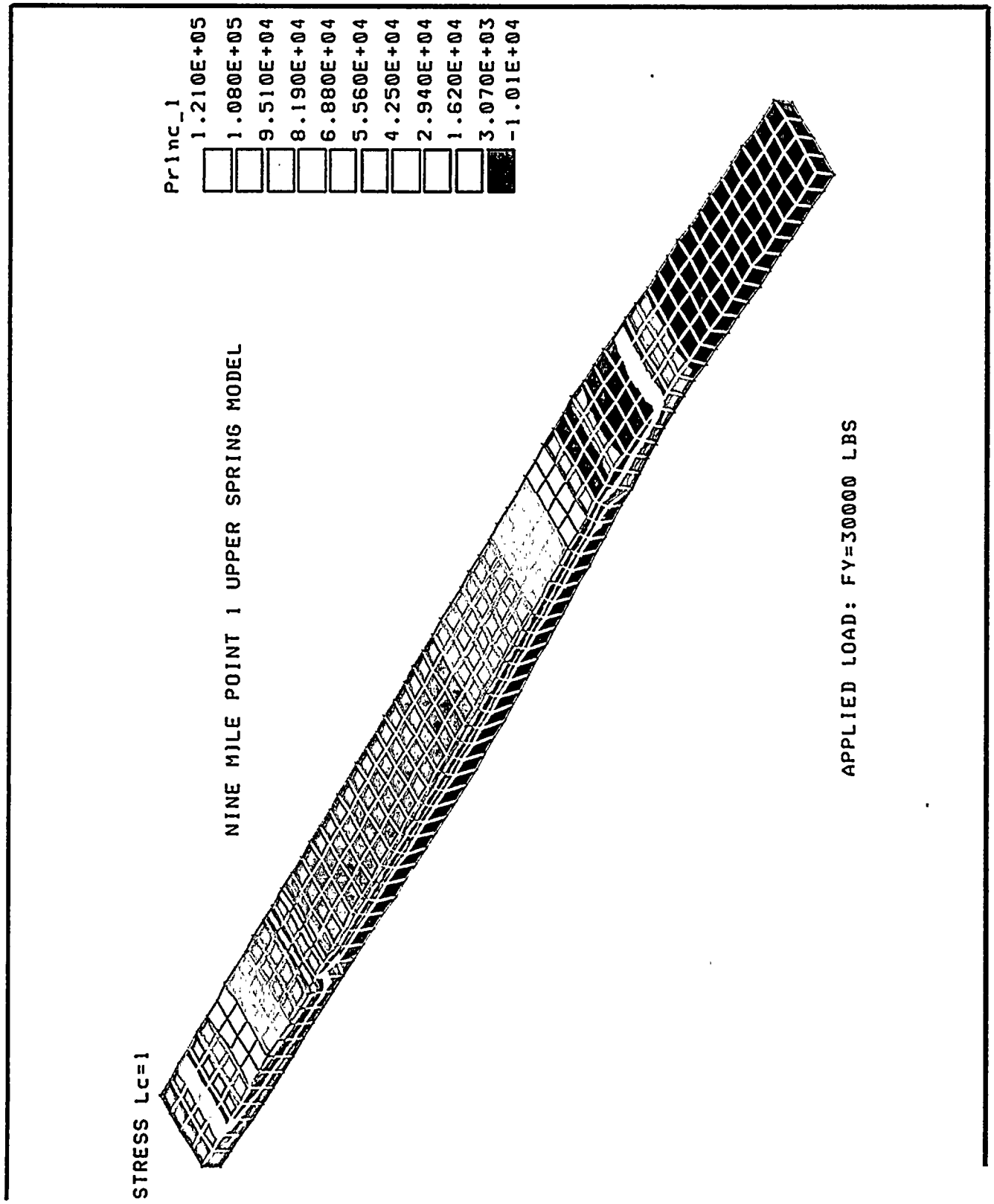

Figure 4-13: Shroud Upper Spring Principal Stress Distribution Due to a Figurative Load of 30,000 lb.

The upper spring's linear spring constant extracted from the detailed model is used in the global model to represent this spring. To calculate the proper actual maximum stresses, the maximum stresses extracted from this model are prorated with actual loads extracted from the global model. Table 4-1 summarizes the stresses for different critical load cases and compares them with appropriate allowable stresses.

As is seen in Table 4-1, all stresses for the critical load combinations are below the corresponding allowables. Therefore, upper spring structural integrity is maintained for all circumstances. $P_m + P_b + Q$ stresses were also studied for fatigue analysis. The results showed that the fatigue impact is negligible.

4.8 Shroud Lower Spring Stress Evaluation

The shroud lower spring consists of a diapason-like structure with the fork handle on a simple support, one branch hinged at the location of connection with the vessel and the other branch under the load representing the transmitted shroud side load at its point of connection. To evaluate the linear spring constant and stress values, a finite element model was made with solid elements, as shown in Figure 4-4. The model is assumed hinged at the support locations and under a figurative perpendicular load of 80,000 lbs at the location of contact with the shroud. Figure 4-14 shows the distribution of principal stress in the hardware.

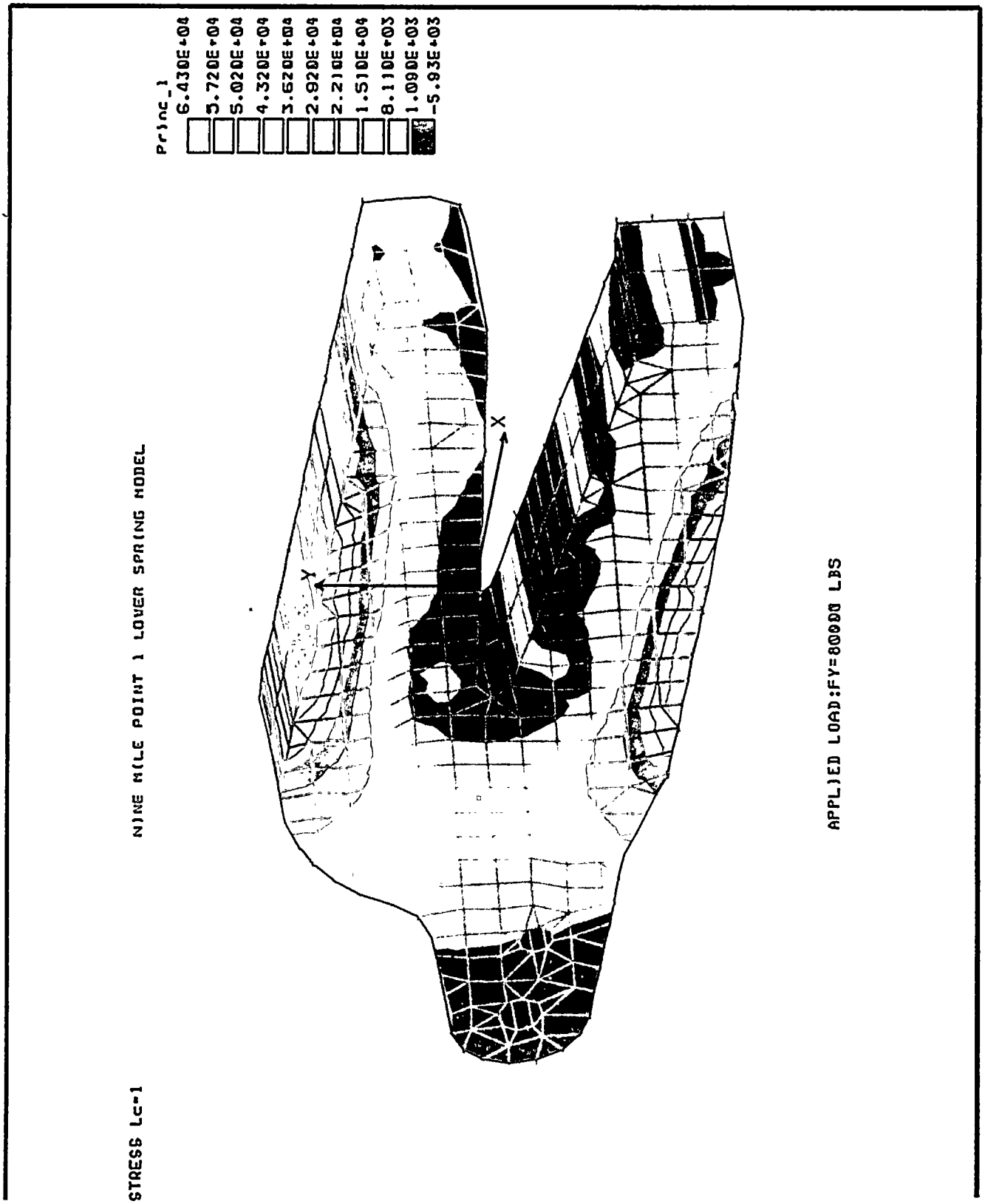

Figure 4-14: Shroud Lower Spring Principal Stress Distribution Due to a Figurative Load of 80,000 lb.

The lower spring's linear spring constant extracted from the detailed model is used in the global model to represent this spring. To calculate the proper actual maximum stresses, the maximum stresses extracted from the detailed model are prorated with actual loads extracted from the global model. Table 4-2 summarizes the stresses in the lower spring for different critical load cases and compares them with appropriate allowable stresses.

As is seen in Table 4-2, all stresses for the critical load combinations are below the corresponding allowables. Therefore, lower spring structural integrity is maintained for all circumstances. $P_m + P_b + Q$ stresses were also studied for fatigue analysis. The results showed that the fatigue impact is negligible.

4.9 Tie Rod Upper Support Stress Evaluation

The upper part of the upper support hangs on the shroud flange. The tie rod is connected to the lower part of this support. To evaluate the linear spring constant and stress values, a finite element model was made with solid elements, as shown in Figure 4-7. The model was assumed fixed at its seat on the shroud flange and hinged at the shroud connection. This model was subjected to an arbitrary load of 137,500 lbs at the proper location to represent the tie rod force. Figure 4-15 shows the distribution of principal stress due to the applied vertical loading.

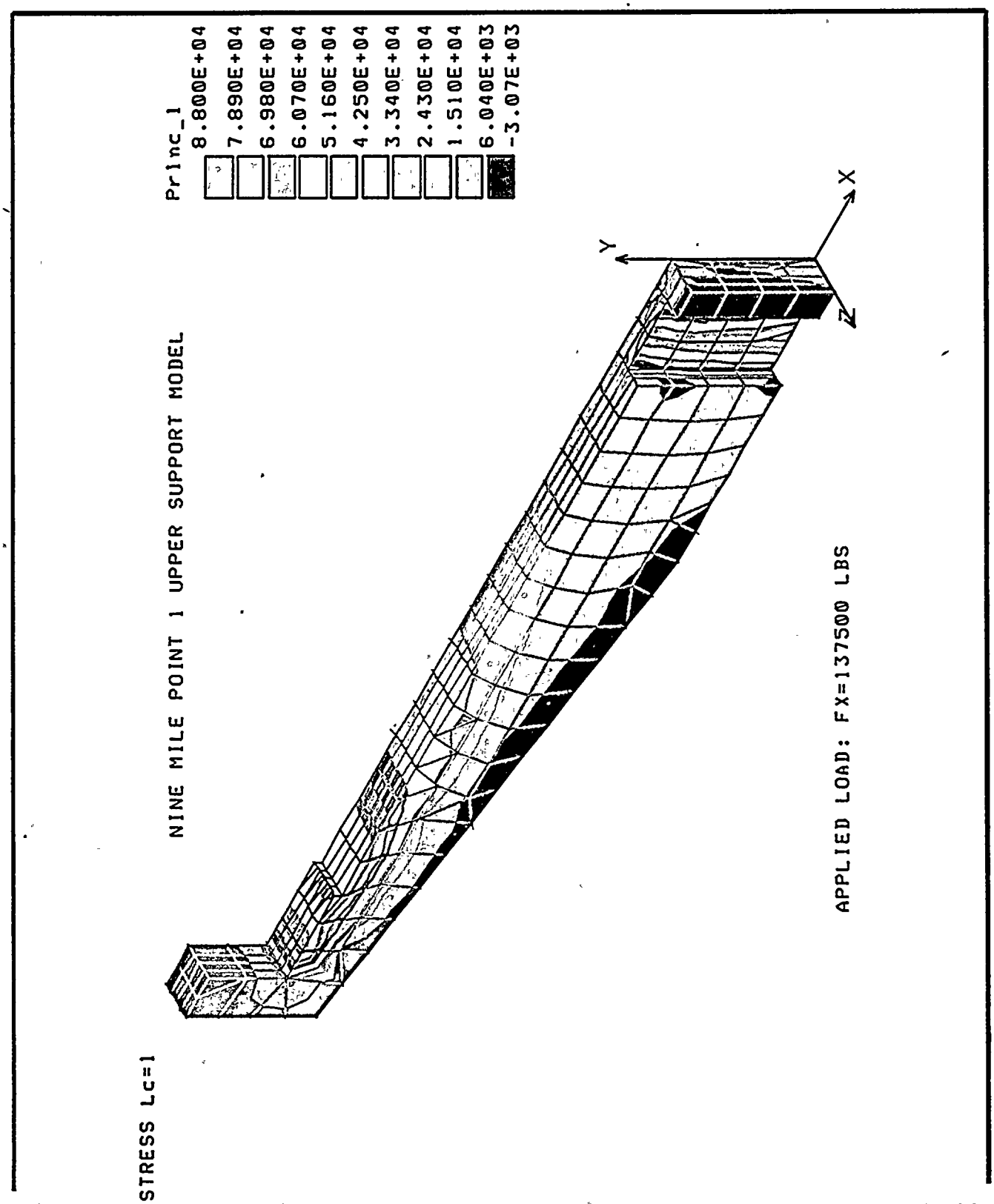

Figure 4-15: Tie Rod Upper Support Principal Stress Distribution Due to a Vertical Load of 137,500 lb.

The lower spring linear spring constant extracted from the detailed model is used in the global model to represent this spring. To calculate the proper actual maximum stresses, the maximum stresses extracted from this model are prorated with actual loads extracted from the global model. Table 4-3 summarizes the stresses in the upper support for different critical load cases and compares them with appropriate allowable stresses.

As is seen in Table 4-3, all stresses for the critical load combinations are below the corresponding allowables. Therefore, upper support structural integrity is maintained for all circumstances. $P_m + P_b + Q$ stresses were also studied for fatigue analysis. The results showed that the fatigue impact is negligible.

4.10 Tie Rod C-Spring Stress Evaluation

The tie rod C-spring used to tie down the shroud consists of a C-shaped structure. To evaluate the linear spring constant and stress values, a finite element model was made with solid elements, as shown in Figure 4-10. The model was assumed hinged at the top connection to the tie rod and under an arbitrary downward load of 275,000 lbs on its bottom connection to the toggle bolts. Figure 4-16 shows the distribution of principal stress.

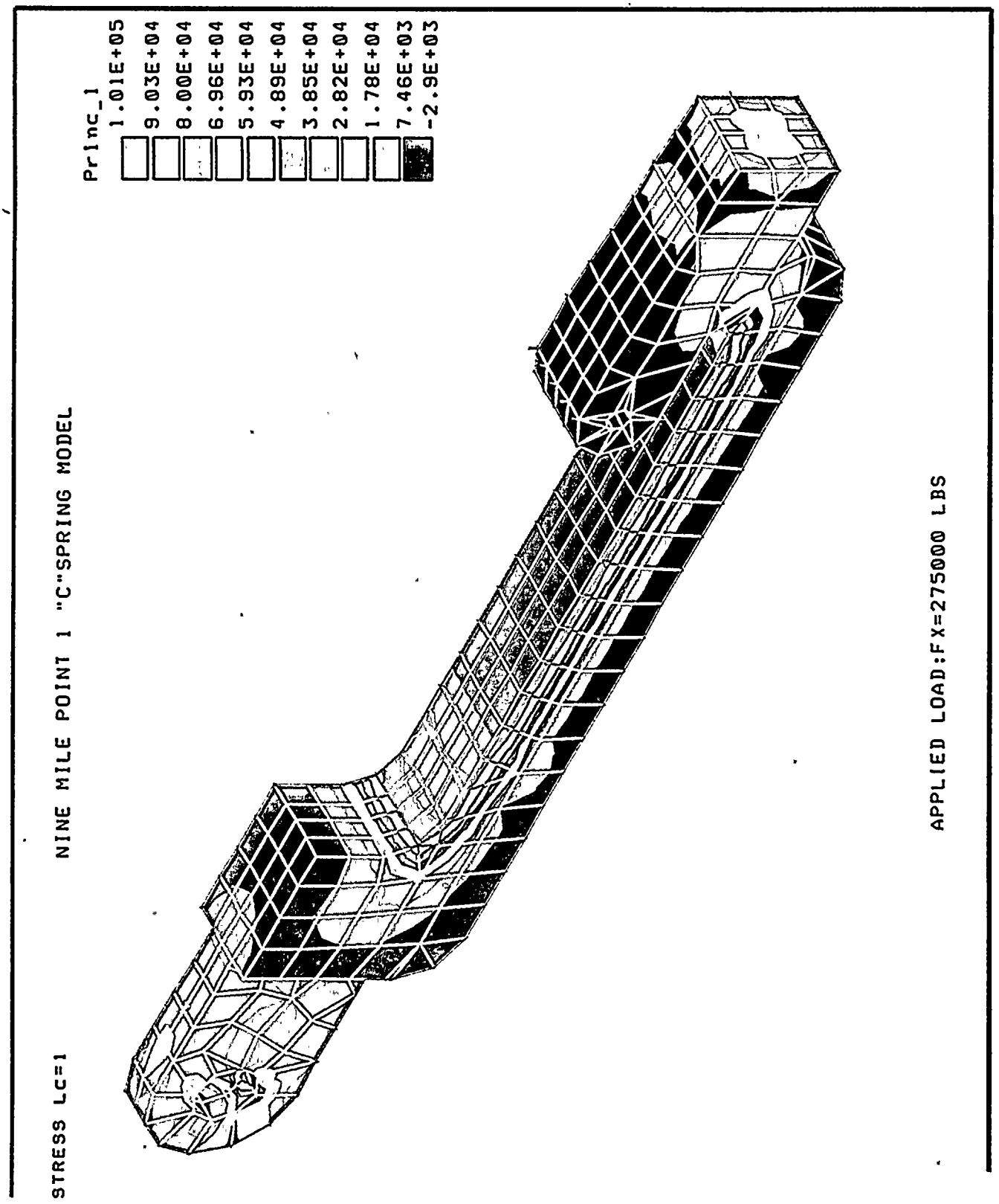

Figure 4-16: Tie Rod C-Spring Principal Stress Distribution Due to a Figurative Vertical Load of 275,000 lb.

The C-spring's linear spring constant extracted from the detailed model is used in the global model to represent this spring. To calculate the proper actual maximum stresses, the maximum stresses extracted from this model are prorated with actual loads extracted from the global model. Table 4-4 summarizes the stresses in the C-spring for different critical load cases and compares them with appropriate allowable stresses.

As is seen in Table 4-4, all stresses for all critical load combinations are below the corresponding allowables. Therefore, C-spring structural integrity is maintained at all circumstances. $P_m + P_b + Q$ stresses were also studied for fatigue analysis. The results showed that the fatigue impact is negligible.

4.11 Shroud Stress Evaluation for Model 1 (H8 Intact)

The stresses in the shroud at critical locations, when H8 is intact, are extracted from the finite element analysis. The results are considered to be conservative since the stresses correspond to nodes under point load application. Also, conservatively, a stress of 1000 psi has been added to all stresses irrespective of their sign to account for the hydrostatic pressure in the RPV.

The following figures have been selected to show some of the results of the finite element analysis. Figure 4-17 shows the shroud principal stress distribution under the normal operating condition. This figure also depicts the meshing refinement of the model including the tie rod, upper and lower spring truss elements. Figures 4-18 and 4-19 show the

shroud displacement distribution and the shroud deflection, respectively, under the Faulted 1 condition.

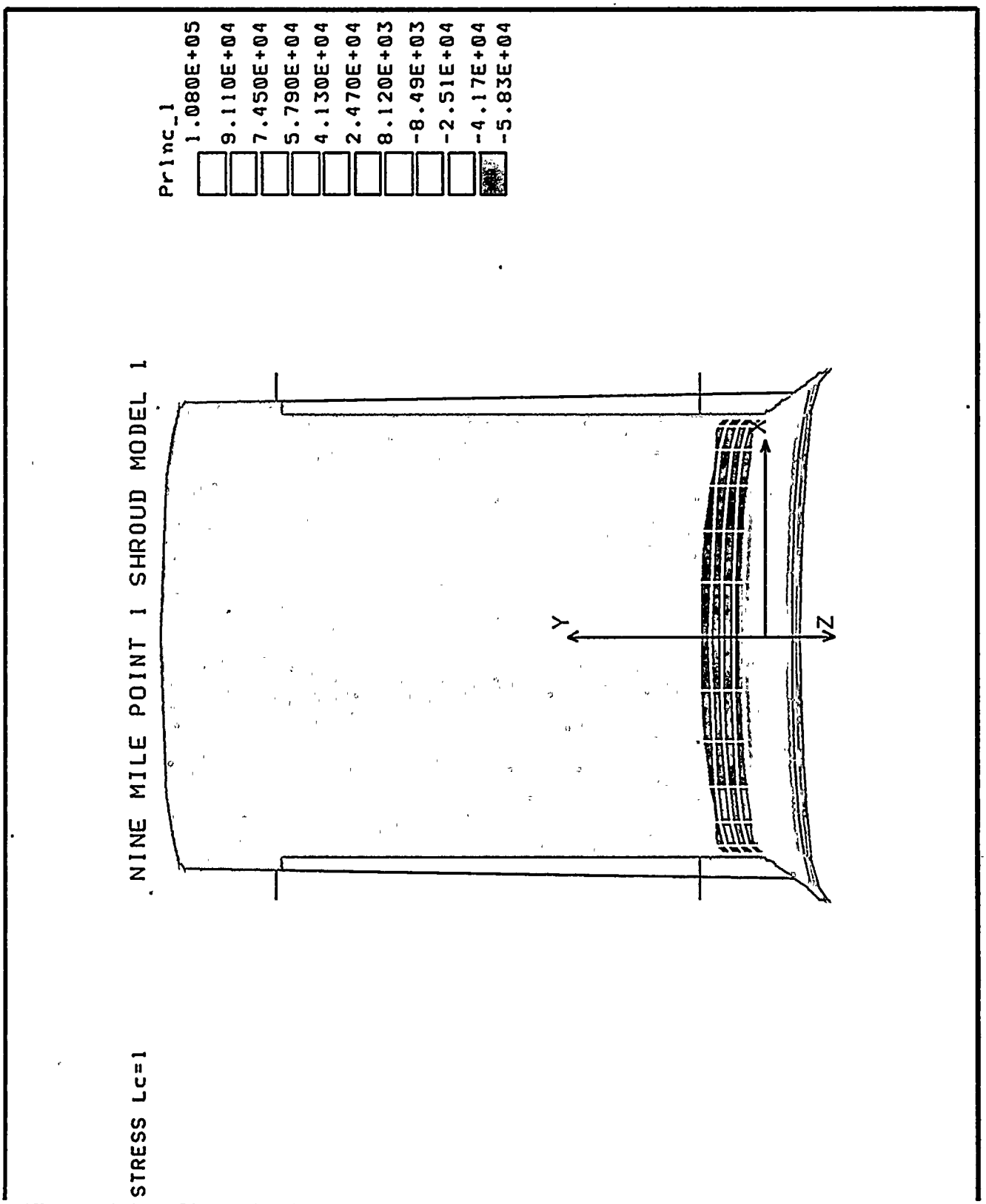

Figure 4-17: Shroud Principal Stress Distribution Contour Under Normal Operating Condition (Model 1, H8 Intact)

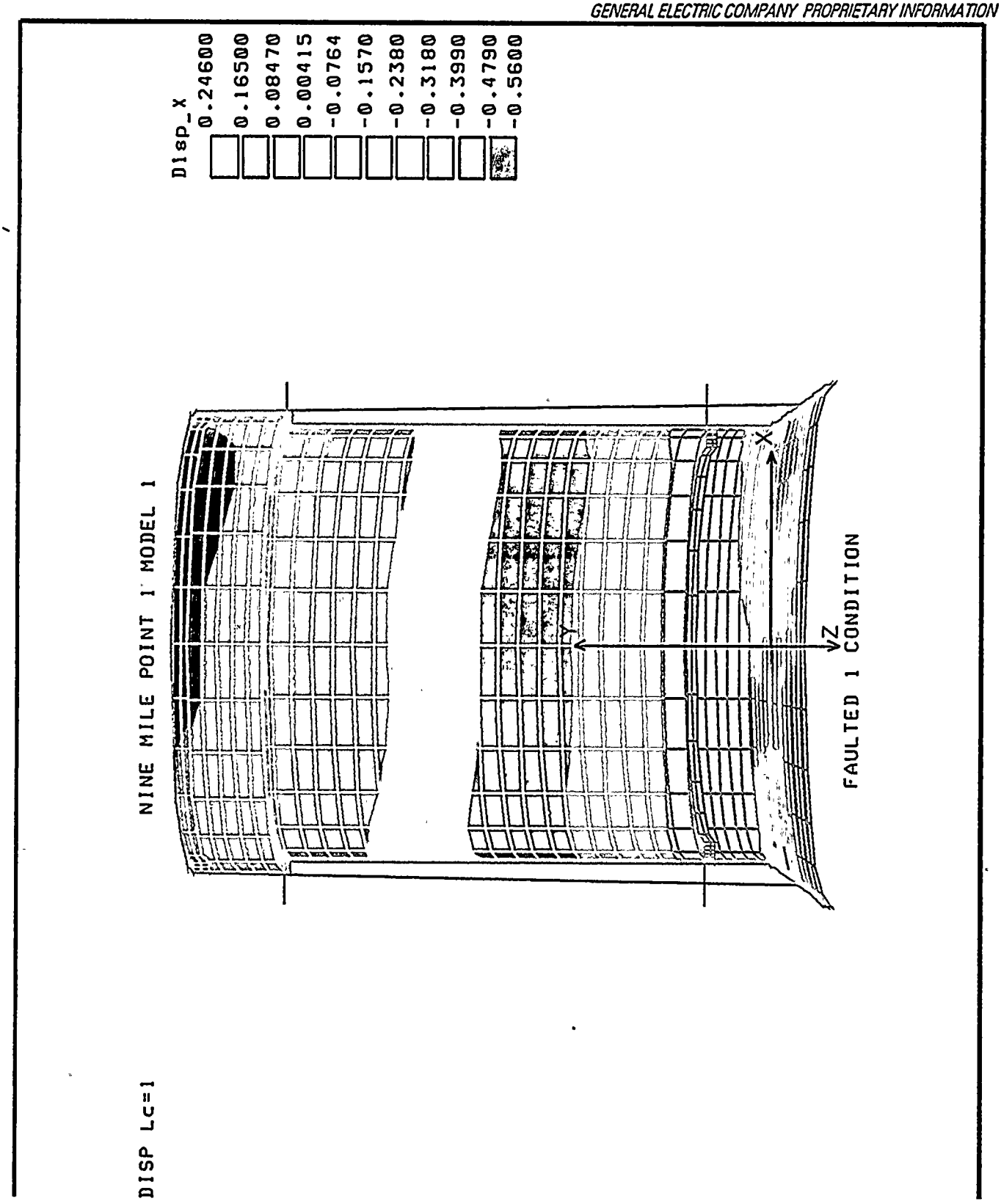

Figure 4-18: Shroud x-Displacement Distribution Contour Under Faulted 1 Condition (Model 1, H8 Intact)

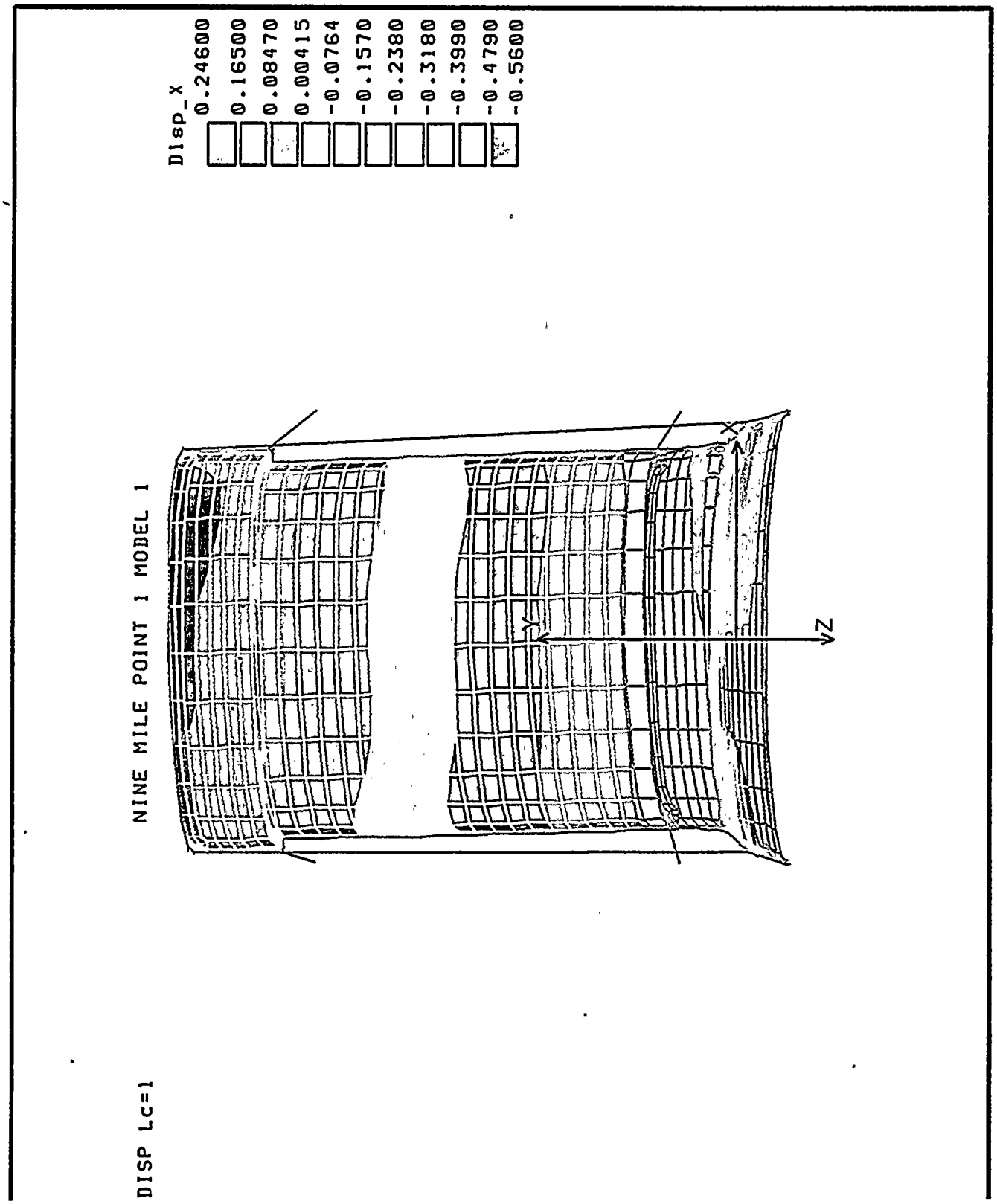

Figure 4-19: Shroud Deflection Plot Under Faulted 1 Condition (Model 1, H8 Intact)

4.11.1 Shroud Stress Evaluation at Upper Support Location (Model 1, H8 Intact)

The stresses at the area of the connection of the tie rods to the shroud head flange are given in Table 4-5.

Table 4-5 shows that all stresses for all critical load combinations are below the corresponding allowables. $P_m + P_b + Q$ stresses were also studied for fatigue analysis. The results showed that the fatigue impact is negligible.

4.11.2 Shroud Stress Evaluation at Upper Spring Location (Model 1, H8 Intact)

The stresses at the area of the connection of the tie rods to the shroud are given in Table 4-6. This connection is at the top guide support ring level.

Table 4-6: Shroud Stress Evaluation at Upper Spring Location (Model 1, H8 Intact)

As is seen in Table 4-6, all stresses for all critical load combinations are below the corresponding allowables. $P_m + P_b + Q$ stresses were also studied for fatigue analysis. The results showed that the fatigue impact is negligible.

4.11.3 Shroud Stress Evaluation at Lower Spring Location (Model 1, H8 Intact)

The stresses at the area of the connection of the lower spring to the shroud are given in Table 4-7. This connection is at the core plate support ring level.

4.12 Shroud Horizontal Displacement Evaluation for Model 1 (H8 Intact)

Table 4-8 recapitulates the critical horizontal displacements of the shroud at top guide and core plate support ring levels. The corresponding allowable displacements are also given for comparison.

4.13 Shroud Structural Integrity Evaluation for Model 1 (H8 Intact)

Based on the results presented in Section 4.11, the shroud maximum stress is below the allowable limit with significant margin. The additional induced fatigue is negligible. Therefore, structural integrity of the shroud is maintained after the proposed repairs.

4.14 Shroud Stress Evaluation for Model 2 (H8 Cracked)

The stresses in the shroud at critical locations, when H8 weld is cracked, are extracted from the finite element analysis. The results are considered to be conservative since the stresses correspond to nodes under point load application. Also, conservatively, a stress of 1000 psi has been added to all stresses irrespective of their sign to account for the hydrostatic pressure in the RPV.

The following figures have been selected to show some of the results of the finite element analysis. Figure 4-20 shows the first principal stress distribution in the shroud for the normal condition. This figure also depicts the meshing refinement of the model including the tie rod, upper and lower spring truss elements. Figures 4-21 and 4-22 show the shroud displacement distribution and the shroud deflection, respectively, under the Faulted 1 condition.

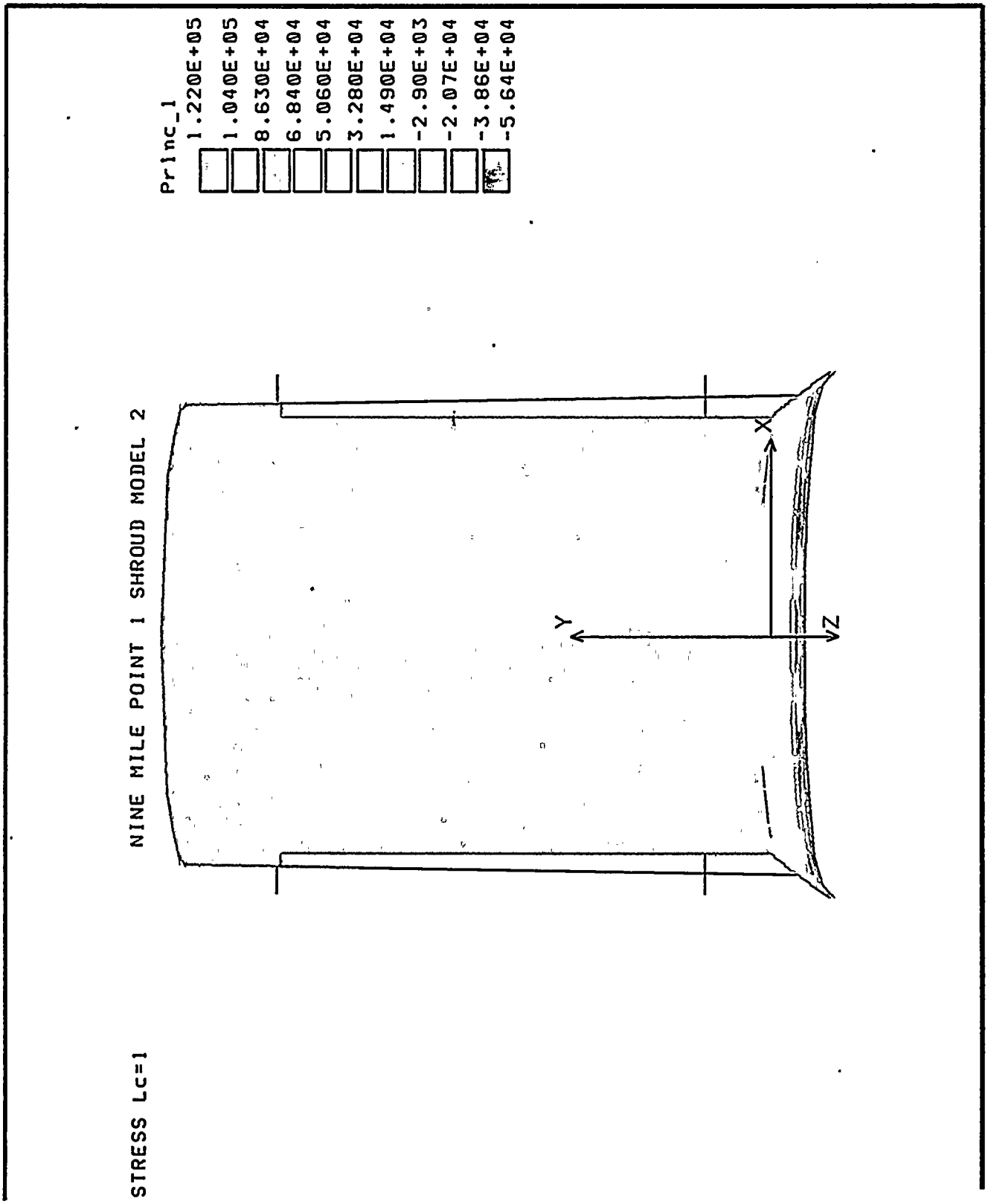

Figure 4-20: Shroud Principal Stress Distribution Contour Under Normal Operating Condition (Model 2, H8 Cracked)

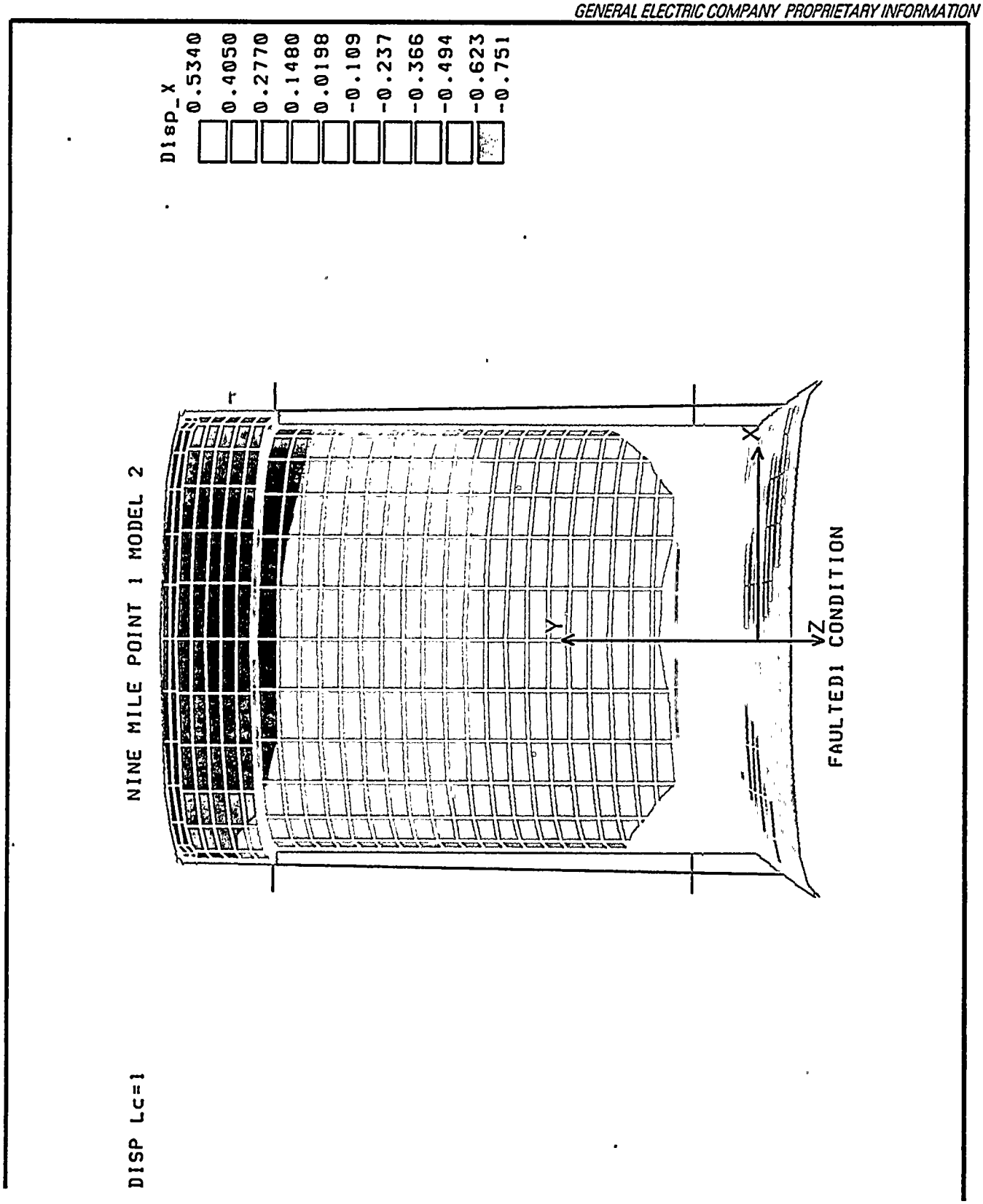

Figure 4-21: Shroud x-Displacement Distribution Contour Under Faulted 1 Condition (Model 2, H8 Cracked)

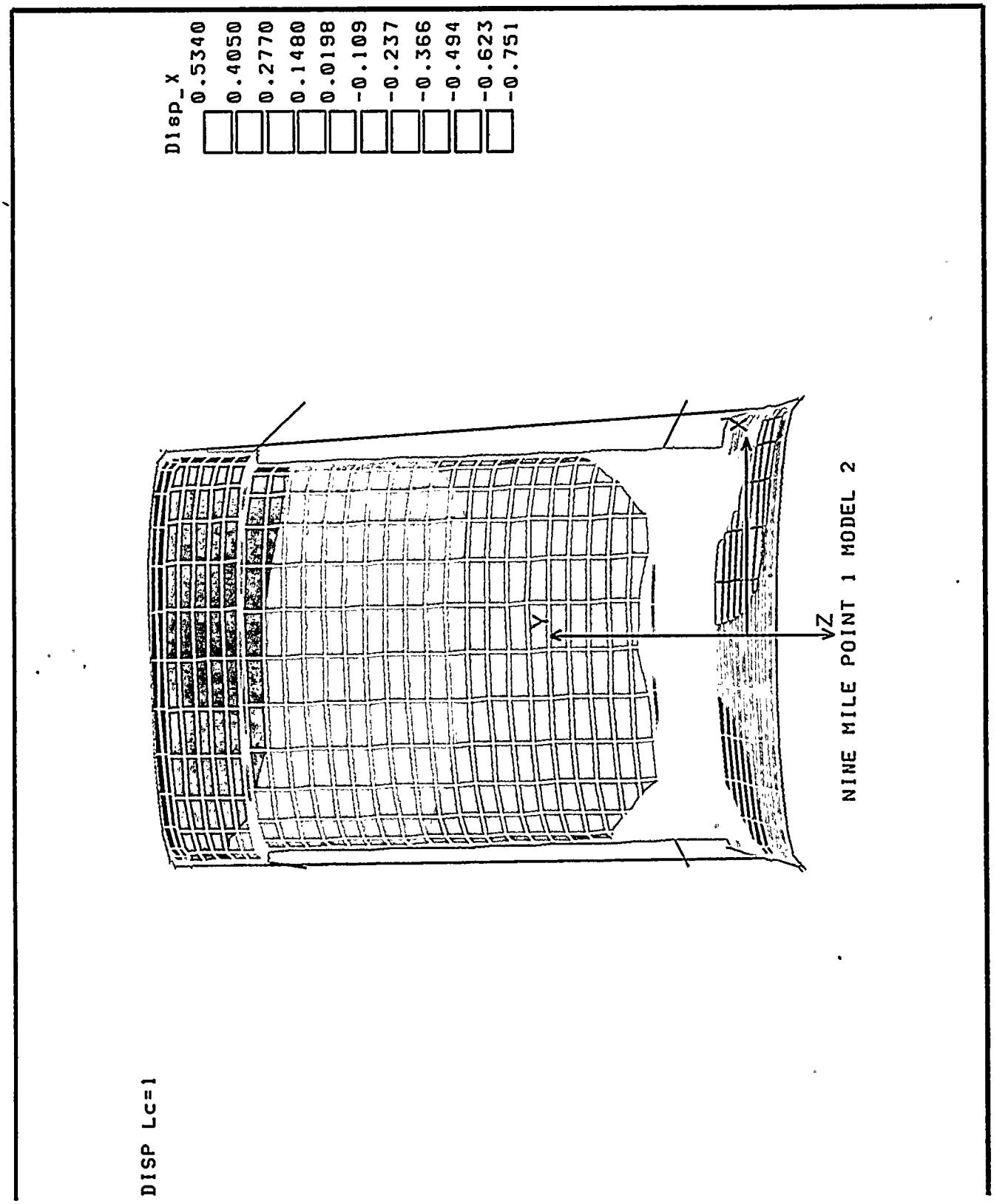

Figure 4-22: Shroud Deflection Plot Under Faulted 1 Condition (Model 2, H8 Cracked)

4.14.1 Shroud Stress Evaluation at Upper Support Location (Model 2, H8 Cracked)

The stresses at the area of the connection of the tie rods to the shroud head flange are given in Table 4-9.

4.14.2 Shroud Stress Evaluation at Upper Spring Location (Model 2, H8 Cracked)

The stresses at the area of the connection of the tie rods to the shroud are given in Table 4-10. This connection is at the top guide support ring level.

As is seen in Table 4-10, all stresses for all critical load combinations are below the corresponding allowables. $P_m + P_b + Q$ stresses were also studied for fatigue analysis. The results showed that the fatigue impact is negligible.

4.14.3 Shroud Stress Evaluation at Lower Spring Location (Model 2, H8 Cracked)

The stresses at the area of the connection of the lower spring to the shroud are given in Table 4-11. This connection is at the core plate support ring level.

4.15 Shroud Horizontal Displacement Evaluation for Model 2 (H8 Cracked)

Table 4-12 recapitulates the critical horizontal displacements of the shroud at top guide and core plate support ring levels. The corresponding allowable displacements are also given for comparison.

4.16 Shroud Structural Integrity Evaluation for Model 2 (H8 Cracked)

Based on the results presented in Section 4.14, the shroud maximum stress is below the allowable limit with significant margin. The additional induced fatigue is negligible. Therefore, structural integrity of the shroud is maintained after the proposed repairs.

5.0 ANALYSIS AND RESULTS: STABILIZERS AND H8 BRACKETS

Detailed hand calculations of the tie rod assemblies and the H8 weld repair brackets were performed for structural analysis purposes to accommodate local areas not covered by the previously described FEA's. The calculations performed are described in the sections which follow.

Material allowable stress values for the components analyzed in this section are as shown in Table 2-3 and allowable stress limits are as shown in Table 2-4.

5.1 Applied Loads

Stabilizer and H8 bracket loads were developed according to operating conditions defined in Reference 1. Load case definitions used in this analysis are shown in Table 2-2. The loads defined for the analysis of the stabilizer, tie rods and lower support bracket are given in Table 3-1. The H8 bracket vertical loads are also given in Table 3-1 for the Emergency #3, Faulted #2 and Faulted #3 cases. These vertical loads include the downward load induced by the pressure difference of -132 psi caused during a recirculation line LOCA, deadweight and applicable seismic forces.

Preload was also accounted for in evaluating the tie rods and toggle bolts. Only the Emergency #3, Faulted #2 and Faulted #3 events were examined since these load cases cause the bounding stresses with respect to the material allowable stresses. In the Emergency #3 case, the components experience a slightly lower load than the Faulted events; however, the allowable stresses for this case are significantly lower than those of the Faulted events. Therefore, both cases were examined. The stress calculations assumed that all of the primary loads transmitted between the H8 repair bracket and the shroud are carried entirely by the bolts and shear pins holding the bracket to the shroud, as would be the case for a bolted joint which has separated (i.e., friction caused by preload was neglected).

Calculations were performed to determine stresses in the shroud, conical support and H8 weld repair bracket for the limiting load conditions. The stresses resulting from these calculations were well within allowable values, thus demonstrating structural acceptability of the shroud attachment location at the H8 weld repair bracket and the repair hardware. The

following sections describe the stress calculations performed for analyzing the repair hardware.

5.2 Evaluation of H8 Weld Bracket

The H8 weld repair bracket analysis involved examining the shroud (locations at which the upper plate attaches to the shroud), the upper plate, and the toggle bolts. Bearing stresses due to the toggle bolt at the shroud hole and upper plate hole were determined and found to be within allowable stress values. The stress caused in the shroud due to the tearout of a toggle bolt was examined and found to be negligible. The bearing of the upper plate on the lower plate of the H8 weld repair bracket was also calculated and compared to the material allowable stresses.

Bending in the foot section of the upper plate was calculated to determine the strength of the foot during a faulted event. An upper bound coefficient of friction of 0.8 was used in this evaluation (as shown in Table 5-1) since a higher coefficient of friction leads to higher applied loads (i.e., this is the opposite of slippage, where a low coefficient would be bounding).

Shear and tearout stress calculations were performed to determine the acceptability of the pins in the toggle bolts with respect to the loads experienced by the pins. The stress calculations performed for the H8 weld repair bracket are shown in Table 5-1. The results indicate that integrity of all components is maintained with significant margin to the material allowables. A summary of the stresses as compared to the material allowable is shown in Table 5-2.

Table 5-1: Emergency and Faulted Events - H8 Bracket Stress Evaluation

Faulted #3 = Case A:
Fvert = 418,833 lb
Fhoriz = 42,715 lb

Faulted #2 = Case A1:
Fvert = 394,897 lb
Fhoriz = 42,715 lb

Emergency #3 = Case B:
Fvert = 324,705 lb

Bolt Preload:
Preload = (T/(K*d)) = 2,954 lb

Shroud:

Bearing @shroud hole:

Sigma(bearing) = Fvert/Ashroud

Ashroud (shear key+toggle) =	8.906	in^2	(2*Dshearkey*tshroud + 2*Dtoggle*tnshroud)
Sigma(bearing) A =	47,027	psi	tnshroud = available thickness on shroud with toggle
Sigma(bearing) A1 =	44,339	psi	- diameters and thicknesses from layout drawing
Sigma(bearing) B =	36,458	psi	
Sy =	18,800	psi (304SS)	
Allowable (A) = 2*1.5*Sy =	56,400	psi	
Allowable (B) = 1.5*1.5*Sy =	42,300	psi	

Shroud tearout stress (Toggle):

Sigma(tearout) = F(h+pr)/Atearout

Atearout =	16.146	in^2	(Perimeter of toggle*tshroud)
Sigma(tearout) A =	2,737	psi	- from toggle bolt dwg 178B3733 rev. 1
Sm =	16,950	psi (304SS)	
Allowable = 2*0.6*Sm =	20,340	psi	

Bearing on shroud (under Toggle head):

Sigma(bearing) = F(h+pr)/Abearing

Abearing =	2.848	in^2	(3*Wprong*tprong + Wprong*hprong)
Sigma(bearing) A =	15,518	psi	- from toggle bolt dwg 178B3733 rev. 1
Sy =	18,800	psi (304SS)	
Allowable (A) = 2*1.5*Sy =	56,400	psi	

Toggle Bolt:

Shear of toggle:

Sigma(shear) = Fvert/4/Ashear

Ashear(4*tprong*Lprong) =	2.893	in^2	- from toggle bolt dwg 178B3733 rev. 1
Sigma(shear) A =	36,194	psi	
Sigma(shear) A1 =	34,125	psi	
Sigma(shear) B =	28,060	psi	
Sm =	47,500	psi (X-750)	
Allowable (A) = 2*0.6*Sm =	57,000	psi	
Allowable (B) = 1.5*0.6*Sm =	42,750	psi	

Bearing of Toggle on Bracket (at hole):

Sigma(bearing) = Fvert/4/Abracket

Abracket(Dtoggle*tbracket) =	11.281	in^2	- from toggle bolt dwg 178B3733 rev. 1 and
Sigma(bearing) A =	9,282	psi	bracket dwg 178B3732 rev. 1
Sigma(bearing) A1 =	8,751	psi	
Sigma(bearing) B =	7,196	psi	
Sy =	92,300	psi (X-750)	
Allowable (A) = 2*Sy =	184,600	psi	
Allowable (B) = 1.5*Sy =	138,450	psi	

Table 5-1: Emergency and Faulted Events - H8 Bracket Stress Evaluation (cont'd)

Faulted #3 = Case A:
Fvert = 418,833 lb
Fhoriz = 42,715 lb

Faulted #2 = Case A1:
Fvert = 394,897 lb
Fhoriz = 42,715 lb

Emergency #3 = Case B:
Fvert = 324,705 lb

Bolt Preload:
Preload = (T/(K*d)) = 2,954 lb

Upper Plate:

Bending in foot section: Coeff. of Friction = 0.8

Sigma(bending) =	Mc/I		
Sigma(shear) =	Fhoriz/Ashear		
Ashear(Lfoot*Wfoot) =	9.332	in^2	- from bracket dwg 178B3732 rev. 1
M =	34,172	in-lb	
c = (h/2) =	0.515	in	
I = (H*h^3/12) =	0.825	in^4	
Sigma(bending+shear) A =	25,909	psi	
Sm =	47,500	psi	(X-750)
Allowable (A) = 2*1.5*Sm =	142,500	psi	
Allowable (B) = 1.5*1.5*Sm =	106,875	psi	

Bearing of Upper Bracket on Lower Bracket:

Sigma(bearing) =	Fvert/Abracket		
Abracket(Lfoot*Wfoot-3*Pi/4*Dtap^2) =	9.000	in^2	- from bracket dwg 178B3732 rev. 1
Sigma(bearing) A =	46,535	psi	
Sigma(bearing) A1 =	43,875	psi	
Sigma(bearing) B =	36,077	psi	
Sy =	92,300	psi	(X-750)
Allowable (A) = 2*1.5*Sy =	276,900	psi	
Allowable (B) = 1.5*1.5*Sy =	207,675	psi	

Pin in Toggle:

Shear (Pin):

Sigma(shear) =	F(h+pr)/Ashear		
Ashear(Dpin^2*Pi/4*2 pins) =	2.193	in^2	- from toggle bolt dwg 178B3733 rev. 1
Sigma(shear) =	20,154	psi	
Sm =	47,500	psi	(X-750)
Allowable (A) = 2*0.6*Sm =	57,000	psi	

Tearout (Pin):

Sigma(tearout) =	F(h+pr)/Atearout		
Atearout(2*Dedge*3*tprong) =	2.680	in^2	- from toggle bolt dwg 178B3733 rev. 1
Sigma(tearout) =	16,491	psi	
Sm =	47,500	psi	(X-750)
Allowable (A) = 2*0.6*Sm =	57,000	psi	

5.3 Evaluation of Stabilizer, Tie Rod and Lower Support

The stabilizer, tie rod assembly and lower support bracket analysis involved examining the conical support (locations at which the tie rod attaches to the conical support), the toggle bolts, the clevis pins and the C-spring ends.

Calculation of bearing stress due to the toggle bolt on the conical support was performed and found to be within the allowable stress values. The stress caused in the conical support due to the tearout of a toggle bolt was also examined and found to be within stress allowables. The primary membrane stresses in the toggle bolts were calculated and compared to the material allowable stresses and found to be acceptable. Shear and tearout stress calculations were performed to determine the acceptability of the pins in the toggle bolts with respect to the loads experienced by the pins.

For the lower support plate, primary membrane and bending stresses were determined and found to be within the material allowable values. The shear stress caused by the loads encountered in the clevis pin were calculated and compared to the material allowable stress. The primary membrane stresses in the C-spring end were calculated and found to be within the stress allowable values.

The overall results indicate that integrity of all components is maintained. A summary of the stresses as compared to the material allowable stresses is shown in Table 5-3 for the limiting load cases. Appendix B of this report provides details of the stress calculations performed.

6.0 FLOW INDUCED VIBRATION

The tie rods are threaded at both ends and are 3.5 inches in diameter and 136.6 inches long. One end is connected with a nut to support the assembly while the other end is threaded to an axial spring member. The spring member is anchored to the reactor vessel support cone by a pin and clevis arrangement. The assembly is thermally preloaded to 79,670 lb. A mid-span support is included which reduces the effective length of the tie rod.

The potential excitation forces come from water flow and from the shroud which has a natural frequency much lower than that of the stabilizer assembly. The stabilizer assemblies are located in the annulus between the shroud and vessel at the 90°, 170°, 270°, and 350° locations. The flow in this region is primarily parallel to the tie rods. The maximum axial flow in the annulus at 105% rated power is calculated to be 5.8 ft/sec. The maximum cross radial flow occurs at the inlet to the recirculation nozzles which flair out on the vessel ID to approximately 40 inches in diameter. The flow velocity at this diameter was estimated to be 9.3 ft/sec. Although there is no stabilizer assembly at this location, the vortex shedding frequency for this flow velocity is only 7 Hz. This is well below the lowest natural frequency of the stabilizer assembly.

6.1 Tie Rod Finite Element Analysis and Natural Frequency

A tie rod finite element model was developed for assessing flow induced vibration using the COSMOS/M software, 1.71 version. The tie rod assembly was modeled as 2-D-beam elements and the element plot is shown in Figure 6-1. Included in the model are the upper support bracket and lower spring both modeled as 2-D beam elements. A conservative tie rod mechanical preload of 3,000 lbs was applied at the upper support bracket. A displacement of 0.01 inch was applied to the end of the lower spring at the reactor pressure vessel (RPV). This corresponds to a preload of 3,000 lbs. In a similar manner, a displacement of 0.07 inches was applied at the upper spring. Gap elements were used at the ends of the lower spring, upper spring & mid-support at the RPV junction. The mid-support was modeled as a rigid link. For the node at the clevis pin,

UX = UY = UZ = ROTX = ROTY = 0. ROTZ = free

For the top of upper support bracket, UY = free. UX = UZ = ROTX = ROTY = ROTZ = 0.

A mode frequency analysis was performed using COSMOS/M. The frequencies for the first five modes are shown in Table 6-1.

Table 6-1: Tie Rod Mode Frequency List

Mode	Frequency (cycles/second)
1	28.16
2	68.30
3	102.15
4	153.60
5	190.95

The natural frequency = 28.16 Hz. This is significantly higher than the forcing frequency (7 Hz) and is considered acceptable.

6.2 H8 Weld Repair Bracket FIV Assessment

An assessment was performed to determine the impact of the H8 weld repair bracket "vibrating" in place on the shroud conical support. This vibration assumes the worst case scenario where the H8 bracket is excited by the vortex shedding frequency of the flow in the downcomer annulus. The vortex shedding frequency was estimated to be 13 Hz in the vicinity of the H8 bracket. It was very conservatively determined that if the H8 bracket "rocked" about two corners, the other two corners would alternately impact at a velocity of 20 ft/sec. Using the bouyant weight of the H8 bracket and an amplification factor corresponding to sudden impact, contact stress calculations were performed for the conical support. The contact stresses resulting from these calculations remained well below handbook allowable values appropriate for contact. Therefore, it was concluded that FIV of the H8 bracket is not a concern even under worst case assumptions.

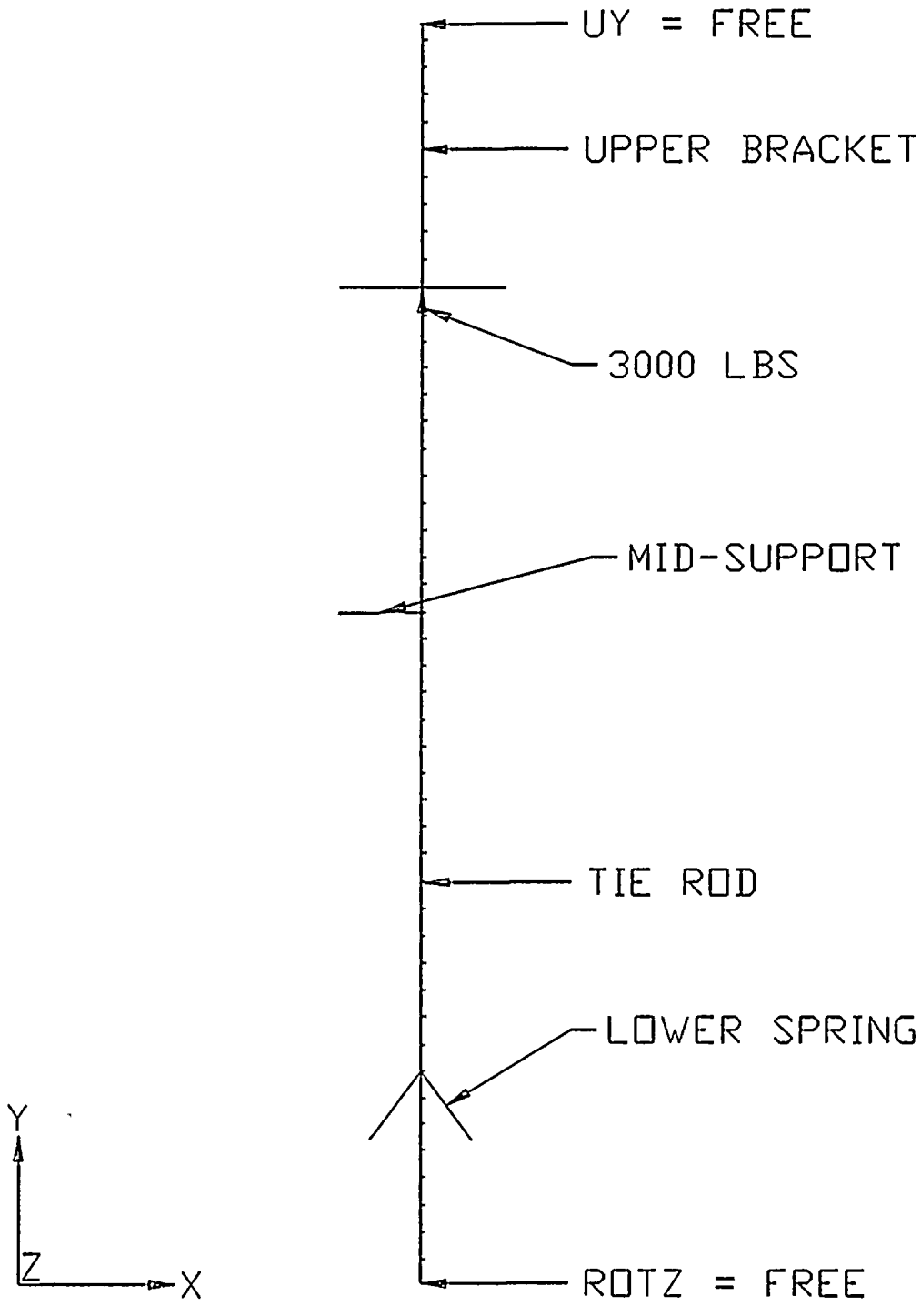

Figure 6-1: FIV Finite Element Model

7.0 CONCLUSIONS

The results of the stress analysis show that the repair design is structurally adequate to withstand the loads imposed during planned and projected operating load conditions. Additionally, stresses at the attachment points of the shroud, in the shroud conical support and vessel/shroud/internals attachment points are all within allowable values. Flow induced vibration was assessed and found to be acceptable, and the impact of the H8 weld bracket on IGSCC susceptibility of the H9 vessel attachment weld was evaluated with acceptable results. It is therefore concluded that the repair design satisfies all of the requirements of Reference 1 and is adequate for permanent, long-term reactor operation as a structural replacement of all welds.

The results documented in this report are conservative for many of the analyzed components. Most notably, the pressure drop associated with the recirculation line break events (ΔP = -132 psig) is extremely conservative based on recent TRACG computer analysis which suggests significantly lower pressure drops for these events (-100 psig or less). Since this large pressure drop contributed to the majority of stresses, significant decreases in stress levels can be expected using the more realistic pressure drops from these recent analyses. Based on this, significant additional stress margins over those shown in this report exist for the components analyzed here.

8.0 REFERENCES

[1] GE Design Specification No. 25A5583, Revision A, "Shroud Repair Hardware," GE Nuclear Energy, San Jose.

[2] G.J. DeSalvo and R.W. Gorman, ANSYS Engineering Analysis System User's Manual, Swanson Analysis Systems, Inc., Houston, PA, Revision 4.4a, May 1, 1989.

[3] Drawings:

a. 105E1413A, Rev. 0, 'Nine Mile Point 1 Shroud Data," GE Nuclear Energy, San Jose, CA.
b. E-231-560-1, Rev. 1, "General Arrangement Elevation," Combustion Engineering, Chattanooga, TN.
c. 237E433, Rev. 9, "Reactor Vessel," GE Nuclear Energy, San Jose, CA.
d. 706E231, Rev. 5, "Shroud," GE Nuclear Energy, San Jose, CA.

[4] ASME Boiler and Pressure Vessel Code, Section III, Appendices, 1989 Edition, ASME, New York.

[5] "GE BWR Plant Materials Handbook," GE Nuclear Energy, San Jose, 1993.

[6] GE-NE-B13-01739-03, Seismic Analysis, Core Shroud Repair Modification, Nine Mile Point 1 Nuclear Power Station.

[7] Letter to Roy Corieri and George Inch from J.A Villalta and A. Mahadevan, Subject: Displacement of the Nine Mile Unit 1 Shroud due to DBE and Recirculation Line Break, Dated September 26, 1994.

[8] GE Stress Report 24A6426, Revision 1, "Reactor Pressure Vessel," 12/19/94.

[9] Letter from B. M. Gordon (GE) to J. D. Lazarus, et. al., 'Suitability of Nine Mile Point 1 H8 Shroud Weld Repair Bracket," January 10, 1995.

APPENDIX A: IMPACT OF TIE ROD ASSEMBLY ON H8 WELD STRESSES

A.1 Purpose

The purpose of this assessment is to determine the impact of the tie rod assembly on the stresses at the H8 weld assuming the shroud is in its original (i.e., uncracked) condition. This evaluation applies to normal operating conditions (i.e., steady state).

A.2 Method

In order to perform this assessment, a simplified 2-D model was used. This is reasonable since the 2-D results were first base-lined against the existing 3-D model. The following steps were performed:

(1) A case was run with a 2-D model of *only the vessel and conical support* (to compare with the 3-D model of this same geometry used in Section 3.0). Only the tie rod load acting under normal operating conditions was applied.

(2) The results of step #1 above were compared to the results from the 3-D model described in Section 3.0 for the same loading.

(3) By comparing the results of steps #1 and #2 above, an appropriate scaling factor was determined to apply to the 2-D results. This allowed assessment of the impact on the H8 weld with reasonable results using only a 2-D model.

(4) Two cases were run using the 2-D model, *including the shroud support ring and lower shroud portion in the model* (i.e., H8 weld intact): (i) one case with all normal operating loads, and (ii) one case with all normal operating loads PLUS the tie rod load during normal operating conditions. By comparing these two cases, including modification for the 2-D versus 3-D models, the impact of stresses at the H8 weld was determined.

A.3 Evaluation

A total of four cases were run on the two different 2-D models, as well as one case on the previously developed 3-D model as follows:

Case No.	Model	Description
1	2-D (#1)	Intact shroud, normal operating loads
2	2-D (#1)	Intact shroud, normal operating loads + normal tie rod preload
3	2-D (#1)	Intact shroud, normal tie rod preload only
4	2-D (#2)	Vessel & conical support only, normal tie rod preload only
5	3-D	Normal tie rod preload only *(vessel & conical support only)*

Normal operating loads consisted of:

ΔP_{cono} = 19.2 psig
$P_{reactor}$ = 1,026 psig
$T_{reactor}$ = 546°F
Vessel blow-off load, P_{bo} = 7,232 psi
(for $P_{reactor}$ = 1,000 psig)
Deadweight, DW ≈ 175,000 lb
Shroud blow-off load, F_{bo} = 308,000 lb
Normal tie rod preload, F_{tr} = 61,680 lb/rod x 4 tie rods

NOTE: IT IS REALIZED THAT SOME OF THE ABOVE LOADS ARE SLIGHTLY DIFFERENT FROM THE ACTUAL APPLIED LOADS; HOWEVER, THEY ARE THE CORRECT ORDER OF MAGNITUDE AND ARE USED IN A COMPARATIVE MANNER, SO ANY CHANGES IN THEIR VALUES ARE JUDGED TO NOT INFLUENCE THE RESULTS PRESENTED HERE SIGNIFICANTLY.

The DW, shroud blow-off, and tie rod loads were applied as a pressure to the top of the shroud as follows:

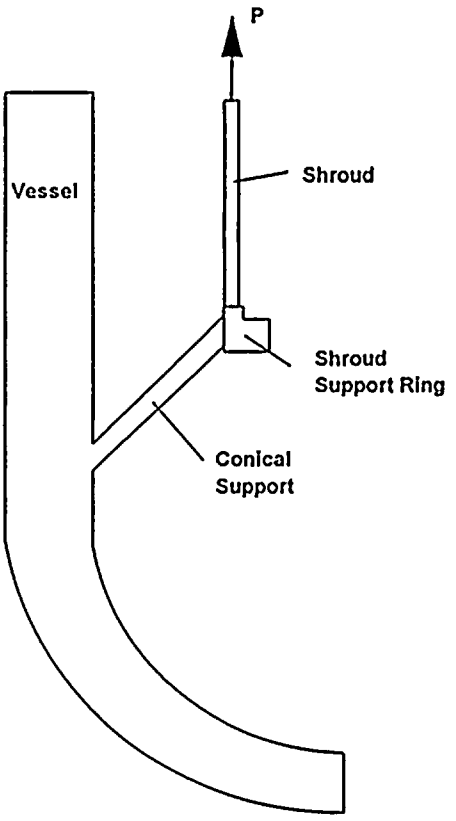

$$P = F/A = (F_{bo} - DW - F_{tr})/(\pi D_m t)$$

Note: F_{tr} and DW act downward, F_{bo} acts upward; thus, + = upward.

F_{tr} was only included in the shroud blow-off load for cases #2 and #3; for all other cases, either the shroud was not modeled (so no blow-off load was necessary), or the tie rod load was not applied (so F_{tr} was set to 0). For all cases where the tie rod load was included, the tie rod load was applied in the upward direction on the conical support, distributed over the nodes where the repair hardware contacted the conical support on its lower surface.

NOTE: EVEN THOUGH THE TIE ROD ACTS AT 4 'POINTS' ON THE TOP OF THE SHROUD, THE 'SMEARING' OF THE LOAD EFFECTIVELY DONE BY THE ABOVE EQUATION WAS JUDGED ADEQUATE FOR THE H8 WELD REGION SINCE THE LOAD WILL 'SPREAD-OUT' OVER THE HEIGHT OF THE SHROUD (i.e., this distance is well over three attenuation lengths).

For F_{tr} as applied to a 2-D model, the following was applied:

$$F_{tr} = (61{,}680 \times 4)/(2\pi) \text{ lb/radian}$$

NOTE: THE ABOVE LOAD BALANCES OUT THE LOAD APPLIED AT THE TOP OF THE SHROUD (EQUILIBRIUM!); HOWEVER, IT MAY NOT ACCURATELY SIMULATE THE 'POINT' LOADING EFFECT ON THE CONICAL SUPPORT. THEREFORE, A SCALING FACTOR BASED ON A COMPARISON OF THE 2-D MODEL VERSUS THE 3-D MODEL (i.e., case #4 versus case #5) WAS DETERMINED FOR APPLICATION TO THE RESULTS.

A.4 Results

The final results and the impact on the H8 weld are contained in Table A-1.

Table A-1: Stress Summary of Tie Rod Impact on H8 Weld

Scaling Factor = 1.00 = CASE #5/CASE #4

Load Case	Surface	ANSYS Linearized Stress Results (SI) Membrane Stress (psi)	Membrane + Bending Stress (psi)	Total Stress (psi)	
Without Tie Rod (ALL LOADS)	Top	8,780	13,200	30,760	CASE #1
	Mid	8,780	8,690	24,390	
	Bottom	8,780	7,207	22,440	
With Tie Rod (ALL LOADS)	Top	8,234	12,610	30,320	CASE #2
	Mid	8,234	8,130	24,070	
	Bottom	8,234	6,748	22,450	
With Tie Rod (ONLY TIE ROD LOAD)	Top	4,437	9,240	28,230	CASE #3
	Mid	4,437	4,303	22,600	
	Bottom	4,437	5,826	23,760	
SCALED (ONLY TIE ROD LOAD)	Top	4,437	9,240	28,230	= Scaled Case #3
	Mid	4,437	4,303	22,600	
	Bottom	4,437	5,826	23,760	
With Tie Rod (REVISED ALL LOADS)	Top	8,234	12,610	30,320	= Case #2 - Case #3
	Mid	8,234	8,130	24,070	+ Scaled Case #3
	Bottom	8,234	6,748	22,450	
Difference	Top	-6.22%	-4.47%	-1.43%	= Change between Case #1
	Mid	-6.22%	-6.44%	-1.31%	and REVISED ALL LOADS
	Bottom	-6.22%	-6.37%	0.04%	
Max. Diff. (%)		-6.22%	-4.47%	0.04%	
Min. Diff. (%)		-6.22%	-6.44%	-1.43%	

A.5 Conclusion

The results from Table A-1 demonstrate that the maximum impact of the installed tie rod during normal operating conditions on stress intensity is approximately 0.04% (increase in total stress intensity) or -6.44% (decrease in membrane + bending stress intensity). The membrane stress intensity decreases by 6.22%. With the exception of the total stress intensity that increases very slightly on one surface, all stress intensities actually drop a small amount as a result of tie rod preload.

This impact is considered to be minimal and therefore verifies that the tie rod has an insignificant impact on the existing H8 weld.

APPENDIX B: STABILIZER HARDWARE STRESS CALCULATIONS

B.1 Summary of Stabilizer Hardware Stress Calculations

The results of the hardware stress calculations are summarized below. The stresses are determined as a function of the tie rod load (TRL).

Table B-1: Summary of Bounding Tie Rod Loads

Event	Tie Rod Load (TRL), lb
Normal Operation	79,670
Upset	162,076
Emergency	216,520
Faulted	311,710

Clevis Pin
(112D6549)

The Inconel X-750 clevis pin is loaded in double shear by the tie rod. The pin minimum diameter is 2.998 inches with a minimum area of 7.059 in^2.

Stress = TRL / (2 X area) = TRL / 14.11 in^2

Clevis Pin Shear Stresses

EVENT	CALCULATED STRESS, PSI	ALLOWABLE STRESS, PSI
Normal	5,646	28,500 (0.6 S_m)
Upset	11,475	28,500 (0.6 S_m)
Emergency	15,330	42,750 (1.5 x 0.6S_m)
Faulted	22,070	57,000 (2 x 0.6 S_m)

C-Spring
(112D6567)

The minimum stress area in the Inconel X-750 C-spring is at the attachment of the clevis pin. The minimum stress area is calculated at 7.648 in^2. In this area the part is loaded in tension. The stresses calculated for the C-Spring flexure are calculated by finite element analysis in Section 4.0 of this report.

Stress = P/A = TRL / 7.648 in^2

C-Spring Stresses

EVENT	CALCULATED STRESS, PSI	ALLOWABLE STRESS, PSI
Normal	10,416	47,500 (S_m)
Upset	21,191	47,500 (S_m)
Emergency	28,311	71,250 (1.5 S_m)
Faulted	40,758	95,000 (2 S_m)

Lower Support, Hook
(112D6585)

The clevis pin bears against the hook section of the lower support resulting in both primary membrane and bending stresses. The minimum stress area is 7.102 in^2. The lower support is made of Inconel X-750. The primary plus bending stresses are shown in the table below.

Primary membrane = TRL /2A = TRL / 14.20 in^2

The bending stress = Mc/I, or $6M/bh^2$ for a rectangular section.
"M" is the bending moment = TRL X 3.637 in·
"b" is material thickness and "h" is the depth of the section.

Bending stress = 6 x TRL x 3.637 / (2 x 4.225^2 x 1.68) = TRL / 2.747

Support Hook Stresses

EVENT	CALCULATED STRESS, PSI	ALLOWABLE STRESS, PSI
Normal	34,612	71,250 ($1.5S_m$)
Upset	70,412	71,250 ($1.5S_m$)
Emergency	94,065	106,875 ($2.25S_m$)
Faulted	135,423	142,500 ($3S_m$)

Lower Support, Base
(112D6585)

The Inconel X-750 base is loaded in shear and in bending. The shear and the bending stress are not in the same direction and are evaluated separately.

Bending stress = $6M / bh^2$ (for a rectangular section)
"M" is the bending moment = TRL x 4.10 in / 2

Bending stress = 6 x TRL x 4.10 / (2 x 7.98 in x 2.22 in^2) = TRL / 3.197

Base Bending Stresses

EVENT	CALCULATED STRESS, PSI	ALLOWABLE STRESS, PSI
Normal	24,912	71,250 ($1.5S_m$)
Upset	50,681	71,250 ($1.5S_m$)
Emergency	67,705	106,875 ($2.25S_m$)
Faulted	97,471	142,500 ($3S_m$)

Shear stress = TRL / (2 x area)
Shear stress = TRL / 35.46 in^2

Base Shear Stresses

EVENT	CALCULATED STRESS, PSI	ALLOWABLE STRESS, PSI
Normal	2,246	28,500 ($0.6S_m$)
Upset	4,570	28,500 ($0.6S_m$)
Emergency	6,110	42,750 ($1.5 \times .0.6S_m$)
Faulted	8,800	57,000 ($2 \times 0.6S_m$)

Toggle Bolt
(112D6580)

Two Inconel X-750 toggle bolts share the tie rod load and are loaded in tension. The minimum area is at the intersection of the slot through the bolt and the hole for the toggle pin. The minimum stress area is 1.976 in^2.

Stress = TRL / (2 x area) = TRL / 3.952 in^2

Toggle Bolt Stresses

EVENT	CALCULATED STRESS, PSI	ALLOWABLE STRESS, PSI
Normal	20,160	47,500 (S_m)
Upset	41,011	47,500 (S_m)
Emergency	54,787	72,250 ($1.5S_m$)
Faulted	78,873	95,000 ($2S_m$)

Cone Bearing Load
(112D6581)

The toggle bears on the cone at the edge of the toggle bolt holes. The cone is evaluated since the Inconel 600 allowable stress is less than that of the Inconel X-750 toggle. The minimum bearing area is calculated at 3.261 in^2. The tie rod load is distributed equally between the two toggle bolts. Since the toggle pulls against the tapered cone, the reaction load at the cone is greater than the tie rod load. The load multiplication factor is calculated to be 1/0.74.

Bearing stress = TRL / (2 x 0.74 x 3.261) = TRL / 4.826

Cone Bearing Stresses

EVENT	CALCULATED STRESS, PSI	ALLOWABLE STRESS, PSI
Normal	16,508	42,525 ($1.5S_y$)
Upset	33,583	42,525 ($1.5S_y$)
Emergency	44,865	63,790 ($2.25S_y$)
Faulted	64,589	85,050 ($3S_y$)

Toggle
(112D6581)

The stabilizer load is distributed between two Inconel X-750 toggles. The load tends to shear the at the hole through the part. The minimum shear area is 5.124 in^2.

Shear stress = TRL / (2 x 0.74 x 5.124 in^2) = TRL / 7.584

Toggle Shear Stress

EVENT	CALCULATED STRESS, PSI	ALLOWABLE STRESS, PSI
Normal	10,505	28,500 ($0.6S_m$)
Upset	21,372	28,500 ($0.6S_m$)
Emergency	28,551	42,750 ($1.5 \times 0.6S_m$)
Faulted	41,100	57,000 ($2 \times 0.6S_m$)

Pin, Toggle Bolt
(112D6583)

Two Inconel X-750 toggle pins share the stabilizer load and are loaded in double shear. The minimum shear area is 2.136 in^2.

Shear stress = TRL / ($2 \times 0.74 \times 2 \times 2.136 in^2$) = TRL / 6.322

Toggle Bolt Shear Stress

EVENT	CALCULATED STRESS, PSI	ALLOWABLE STRESS, PSI
Normal	12,600	28,500 ($0.6S_m$)
Upset	25,632	28,500 ($0.6S_m$)
Emergency	34,245	42,750 ($1.5 \times 0.6S_m$)
Faulted	49,300	57,000 ($2 \times 0.6S_m$)

Tie Rod
(112D6547)

The tie rod is 316L stainless steel loaded in tension. The tie rod is 3.5 inches in diameter, but minimum stress area is at the undercut for the threads at each end. The minimum stress area is 8.76 in^2. The allowable stress is based on the certified material properties reports for the particular heat of material (Heat No. 106578) used for the tie rods.

Stress = TRL /Area = TRL / 8.76 in^2

Tie Rod Stresses

EVENT	CALCULATED STRESS, PSI	ALLOWABLE STRESS, PSI
Normal	9,094	22,900 (S_m)
Upset	18,502	22,900 (S_m)
Emergency	24,717	34,350 ($1.5S_m$)
Faulted	35,583	45,800 ($2S_m$)

Mid-Support
(112D6566)

The 316L stainless steel mid-support bracket bears lightly (~200 lb) against the RPV wall. Additional loading may result during a seismic event with H4 and H5 welds failed. The 22,000 lb shroud cylinder would be free to move horizontally and will be restrained by the bracket. The horizontal load to restrain the cylinder during the seismic event is estimated at 2,400 lb. A recirculation line break also results in a side load on the shroud which tends to displace the free cylinder. The side load during the recirculation line break is 17,000 lb which is the limiting load case.

The bearing minimum area of the mid-support is 5.50 in^2.

Bearing Stress = P/A = 17,000 lb / 5.50 in^2 = 3,090 lb/in^2
Allowable stress = $1.5S_y$ = 1.5 x 19,350 psi = 29,025 lb/in^2

Clamp/Spacer
(112D6618)

The 316L stainless steel spacers are located in the annulus between the top of the core support and the shroud. The spacers provide a direct load path from the core support to the shroud in the event the clamping load is not sufficient to carry the horizontal loads. Spacers are in four locations corresponding to the lower spring locations. The possible 63,800 lb horizontal load on the lower spring during a seismic event is the bounding load. The spacer is loaded in bearing and has a minimum bearing area of 5.89 in^2.

Bearing Stress = P/A =63,800 lb / 5.89 in^2 = 10,830 lb/in^2
Allowable Stress = $1.5S_y$ = 1.5 x 19,350 psi = 29,025 lb/in^2

Shroud Head Modification

The cut-outs in the shroud head were evaluated for pressure loads and for the loads during lifting. During lifting, the weight of the shroud head (including the shroud head bolts) is supported at the four lift points. The pressure loads are held by the 36 shroud head bolts. The stresses during lifting are found to be greater than the pressure stressed during normal, upset, emergency and faulted conditions.

Maximum primary plus bending stress = 16,650 lb/in^2
Allowable Stress = $1.5S_m$ = 1.5 x 15,800 lb/in^2 = 23,700 lb/in^2

Core Spray Piping

The core spray piping was modeled and analyzed with the SAP finite element analysis program. The analysis includes a 0.904 inch horizontal shroud movement and a 0.61 inch vertical shroud movement. The maximum strain was calculated at 1% which occurs at the elbow in the riser section of the piping. A 2.5% strain is permissible to prevent material cold-working. Although the 1% strain may result in local plastic deformation, it will not affect the performance of the core spray piping.